Anbar University – Engineering College      Subject: Remote Sensing
Dams and Water resources Eng Dept      Stage: Four
     Dr. Ahmed Saud Mohammed

# The First Lesson

## Concepts and Foundations of Remote Sensing

### 1.1 INTRODUCTION

Remote sensing is the science and art of obtaining information about an object, area, or phenomenon through the analysis of data acquired by a device that is not in contact with the object, area, or phenomenon under investigation. As you read these words, you are employing remote sensing. Your eyes are acting as sensors that respond to the light reflected from this page. The "data" your eyes acquire are impulses corresponding to the amount of light reflected from the dark and light areas on the page. These data are analyzed, or interpreted, in your mental computer to enable you to explain the dark areas on the page as a collection of letters forming words. Beyond this, you recognize that the words form sentences, and you interpret the information that the sentences convey. In many respects, remote sensing can be thought of as a reading process. Using various sensors, we remotely collect data that may be analyzed to obtain information about the objects, areas, or phenomena being investigated. The remotely collected data can be of many forms, including variations in force distributions, acoustic wave distributions, or electromagnetic energy distributions.

## *Overview of the Electromagnetic Remote Sensing Process*

This lecture is about electromagnetic energy sensors that are operated from airborne and space borne platforms to assist in inventorying, mapping, and monitoring earth resources. These sensors acquire data on the way various earth surface features emit and reflect electromagnetic energy, and these data are analyzed to provide information about the resources under investigation. Figure 1.1 schematically illustrates the generalized processes and elements involved in electromagnetic remote sensing of earth resources. The two basic processes involved are data acquisition and data analysis.

The elements of the data acquisition process are :

- energy sources (a),
- propagation of energy through the atmosphere (b),
- energy interactions with earth surface features (c),
- retransmission of energy through the atmosphere (d),
- airborne and/or spaceborne sensors (e),
- resulting in the generation of sensor data in pictorial and/or digital form (f).

In short, we use sensors to record variations in the way earth surface features reflect and emit electromagnetic energy.

The data analysis process :

- (g) involves examining the data using various viewing and interpretation devices to analyze pictorial data and/or a computer to analyze digital sensor data. Reference data about the resources being studied (such as soil maps, crop statistics, or field-check data) are used when and where available to assist in the data analysis. With the aid of the reference data, the analyst extracts information about the type, extent, location, and condition of the various resources over which the sensor data were collected.
- (h), this information is then compiled generally in the form of maps, tables, or digital spatial data that can be merged with other "layers" of information in a geographic information system (GIS). Finally, the information is presented to users (i), who apply it to their decision-making process.
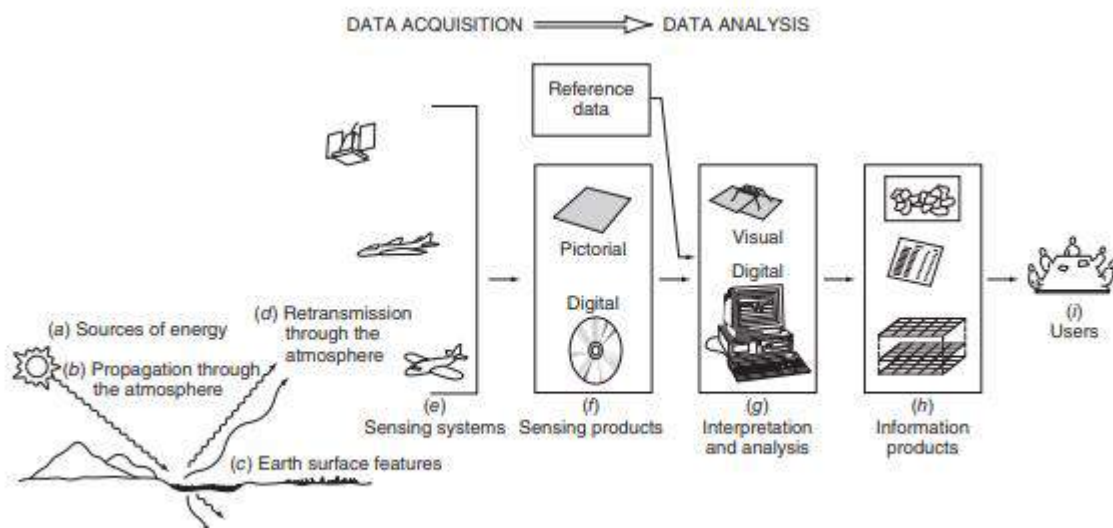


**Figure 1.1** Electromagnetic remote sensing of earth resources.

## 1.2 Energy Sources and Radiation Principles

Visible light is only one of many forms of electromagnetic energy. Radio waves, ultraviolet rays, radiant heat, and X-rays are other familiar forms. All this energy is inherently similar and propagates in accordance with basic wave theory. As shown in Figure 1.2, this theory describes electromagnetic energy as traveling in a harmonic, sinusoidal fashion at the "velocity of light" c. The distance from one wave peak to the next is the wavelength l, and the number of peaks passing a fixed point in space per unit time is the wave frequency v. From basic physics, waves obey the general equation

Anbar University – Engineering College        Subject: Remote Sensing
Dams and Water resources Eng Dept        Stage: Four
        Dr. Ahmed Saud Mohammed

$$c = v\lambda \qquad\qquad (1)$$

Because c is essentially a constant $3*10^8$ m/sec , frequency $v$ and wavelength l for any given wave are related inversely, and either term can be used to characterize a wave. In remote sensing, it is most common to categorize electromagnetic waves by their wavelength location within the electromagnetic spectrum (Figure 1.3). The most prevalent unit used to measure wavelength along the spectrum is the micrometer m . A micrometer equals $1*1^{06}$ m.

Although names (such as "ultraviolet" and "microwave") are generally assigned to regions of the electromagnetic spectrum for convenience, there is no clear-cut dividing line between one nominal spectral region and the next. Divisions of the spectrum have grown from the various methods for sensing each type of radiation more so than from inherent differences in the energy characteristics of various wavelengths. Also, it should be noted that the portions of the electromagnetic spectrum used in remote sensing lie along a continuum characterized by magnitude changes of many powers of 10. Hence, the use of logarithmic plots to depict the electromagnetic spectrum is quite common. The "visible" portion of such a plot is an extremely small one, because the spectral sensitivity of the human eye extends only from about 0.4 $^m$m to approximately 0. 7 $^m$m. The color "blue" is ascribed to the approximate range of 0.4 to 0:5 m, "green" to 0.5 to 0:6 $^m$m, and "red" to 0.6 to 0.7 $^m$m. Ultraviolet (UV) energy adjoins the blue end of the visible portion of the spectrum. Beyond the red end of the visible region are three different categories of infrared (IR) waves: near IR (from 0.7 to 1.3 m), mid IR (from 1.3 to 3 m; also referred to as shortwave IR or SWIR), and thermal IR (beyond 3 to 14 $^m$m, sometimes referred to as longwave IR). At much longer wavelengths (1 mm to 1 m) is the microwave portion of the spectrum.
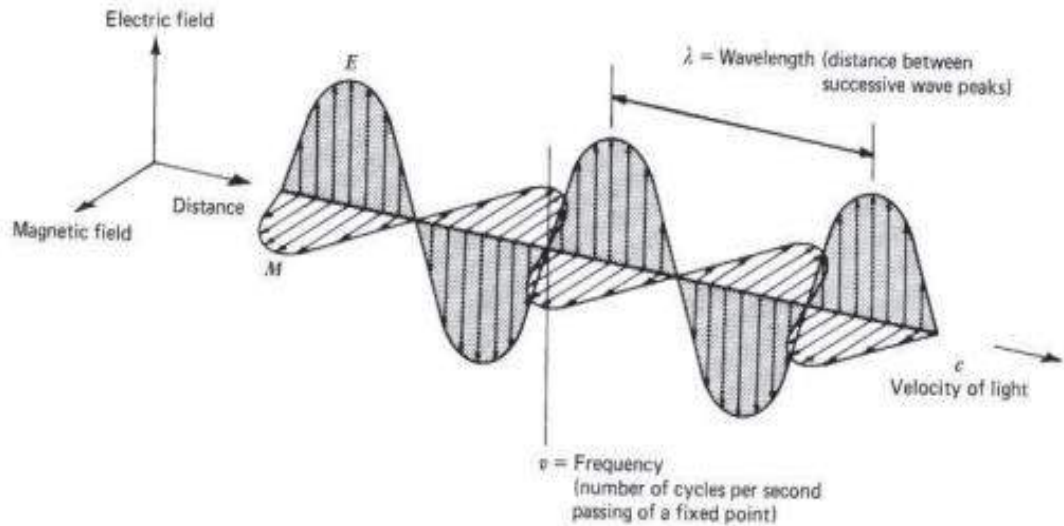
**Figure 1.2** Electromagnetic wave. Components include a sinusoidal electric wave ($E$) and a similar magnetic wave ($M$) at right angles, both being perpendicular to the direction of propagation.
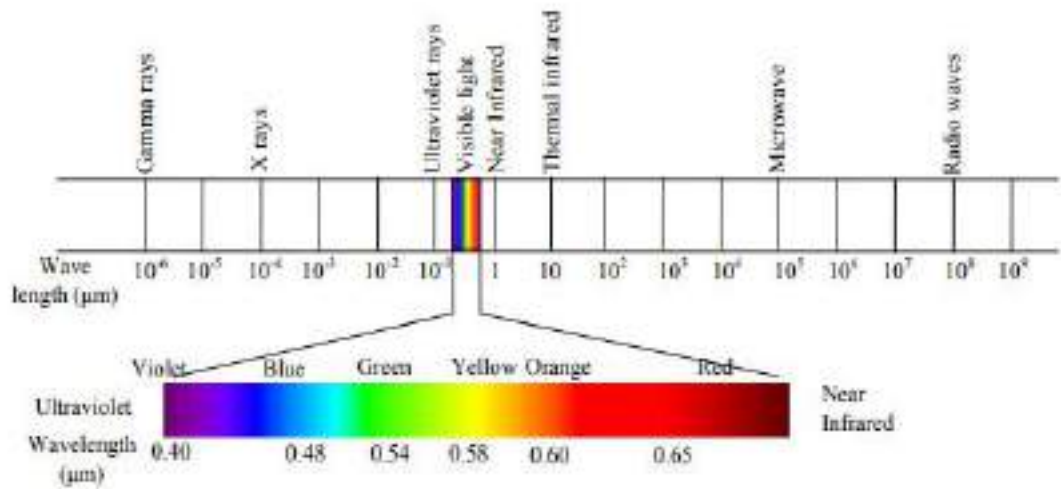


**Figure 1.3** Electromagnetic spectrum.

---------------------------------------------------------------------------------------------------------
# The Second Lesson

## Quantum Energy

Most common sensing systems operate in one or several of the visible, IR, or microwave portions of the spectrum. Within the IR portion of the spectrum, it should be noted that only thermal-IR energy is directly related to the sensation of heat; near- and mid-IR energy are not.

Although many characteristics of electromagnetic radiation are most easily described by wave theory, another theory offers useful insights into how electromagnetic energy interacts with matter. This theory—the particle theory—suggests that electromagnetic radiation is composed of many discrete units called photons or quanta. The energy of a quantum is given as

$$Q = hv \tag{1.2}$$

*where*

$Q$ = energy of a quantum, joules (J)
$h$ = Planck's constant, $6.626 \times 10^{-34}$ J sec
$v$ = frequency

We can relate the wave and quantum models of electromagnetic radiation behavior by solving Eq. 1.1 for $v$ and substituting into Eq. 1.2 to obtain

$$Q = \frac{hc}{\lambda} \tag{1.3}$$

Thus, we see that the energy of a quantum is inversely proportional to its wavelength. The longer the wavelength involved, the lower its energy content. This has important implications in remote sensing from the standpoint that naturally emitted long wavelength radiation, such as microwave emission from terrain features, is more difficult to sense than radiation of shorter wavelengths, such as emitted thermal IR energy. The low energy content of long wavelength radiation means that, in general, systems operating at long wavelengths must "view" large areas of the earth at any given time in order to obtain a detectable energy signal. The sun is the most obvious source of electromagnetic radiation for remote sensing. However, all matter at temperatures above absolute zero (0 K, or -273C) continuously emits electromagnetic radiation. Thus, terrestrial objects are also sources of radiation, although it is of considerably different magnitude and spectral composition than that of the sun. How much energy any object radiates is, among other things, a function of the surface temperature of the object. This property is expressed by the Stefan–Boltzmann law, which states that

$$M = \sigma T^4 \qquad (1.4)$$

*where*

$M$ = total radiant exitance from the surface of a material, watts (W) m$^{-2}$
$\sigma$ = *Stefan–Boltzmann constant*, $5.6697 \times 10^{-8}$ W m$^{-2}$ K$^{-4}$
$T$ = absolute temperature (K) of the emitting material

The particular units and the value of the constant are not critical for the student to remember, yet it is important to note that the total energy emitted from an object varies as T4 and therefore increases very rapidly with increases in temperature. Also, it should be noted that this law is expressed for an energy source that behaves as a blackbody. A blackbody is a hypothetical, ideal radiator that totally absorbs and reemits all energy incident upon it. Actual objects only approach this ideal. Suffice it to say for now that the energy emitted from an object is primarily a function of its temperature, as given by Eq. 1.4.

Just as the total energy emitted by an object varies with temperature, the spectral distribution of the emitted energy also varies. Figure 1.4 shows energy distribution curves for blackbodies at temperatures ranging from 200 to 6000 K. The units on the ordinate scale W m$^{-2}$mm$^{-1}$ express the radiant power coming from a blackbody per 1-mm spectral interval. Hence, the area under these curves equals the total radiant exitance, M, and the curves illustrate graphically what the Stefan–Boltzmann law expresses mathematically: The higher the temperature of the radiator, the greater the total amount of radiation it emits. The curves also show that there is a shift toward shorter wavelengths in the peak of a blackbody radiation distribution as temperature increases. The dominant wavelength, or wavelength at which a blackbody radiation curve reaches a maximum, is related to its temperature by Wien's displacement law,

$$\lambda_m = \frac{A}{T} \qquad (1.5)$$

*where*

$\lambda_m$ = wavelength of maximum spectral radiant exitance, $\mu$m
$A$ = 2898 $\mu$m K
$T$ = temperature, K

Thus, for a blackbody, the wavelength at which the maximum spectral radiant exitance occurs varies inversely with the blackbody's absolute temperature. We observe this phenomenon when a metal body such as a piece of iron is heated. As the object becomes progressively hotter, it begins to glow and its color changes successively to shorter wavelengths—from dull red to orange to yellow and eventually to white. The sun emits radiation in the same manner as a blackbody radiator whose temperature is about 6000 K (Figure 1). Many

Anbar University – Engineering College        Subject: Remote Sensing
Dams and Water resources Eng. Dept.        Stage: Four
Dr. Ahmed Saud Mohammed , Dr. Khamis N. Syle
-----------------------------------------------------------------------------------------------------------------------

incandescent lamps emit radiation typified by a 3000 K blackbody radiation curve. Consequently, incandescent lamps have a relatively low output of blue energy, and they do not have the same spectral constituency as sunlight.
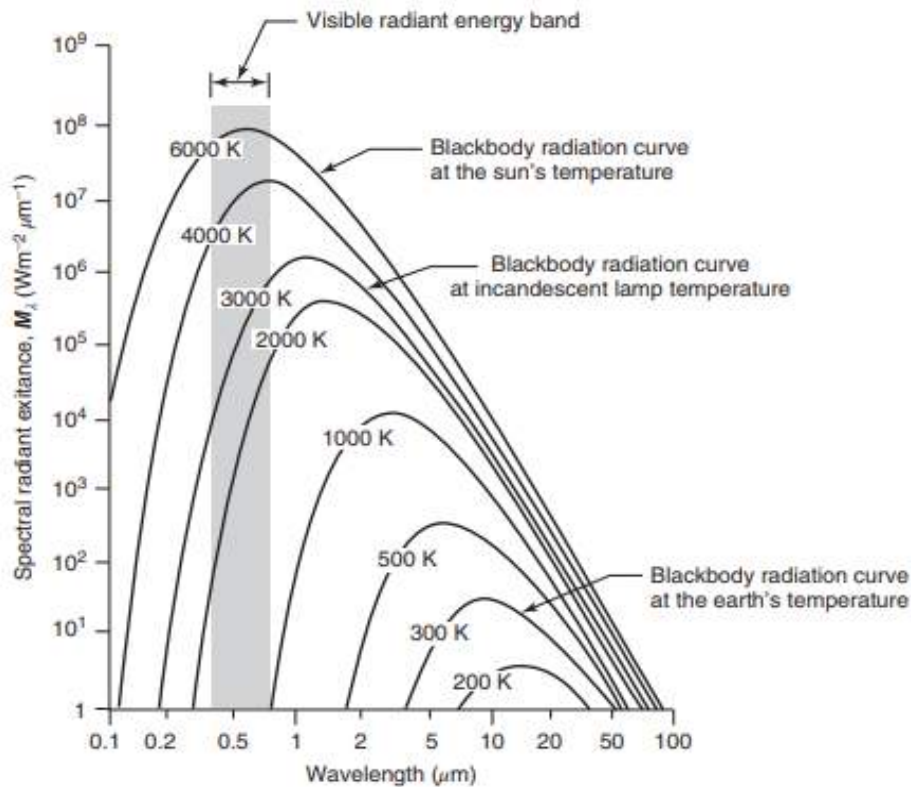


Figure 1: Spectral distribution of energy radiated from blackbodies of various temperatures

The earth's ambient temperature (i.e., the temperature of surface materials such as soil, water, and vegetation) is about 300 K (27°C). From Wien's displacement law, this means the maximum spectral radiant exitance from earth features occurs at a wavelength of about 9.ᵐ7 m. Because this radiation correlates with terrestrial heat, it is termed "thermal infrared" energy. This energy can neither be seen nor photographed, but it can be sensed with such thermal devices as radiometers and. By comparison, the sun has a much higher energy peak that occurs at about 0:5 µm, as indicated in Figure 1.

Our eyes—and photographic sensors—are sensitive to energy of this magnitude and wavelength. Thus, when the sun is present, we can observe earth features by virtue of reflected solar energy. Once again, the longer wavelength energy emitted by ambient earth features can be observed only with a nonphotographic sensing system. The general dividing line between reflected and emitted IR wavelengths is approximately 3 µm.

Anbar University – Engineering College          Subject: Remote Sensing
Dams and Water resources Eng. Dept.          Stage: Four
       Dr. Ahmed Saud Mohammed  , Dr. Khamis N. Syle
-------------------------------------------------------------------------------------------------------------------

Below this wavelength, reflected energy predominates; above it, emitted energy prevails. Certain sensors, such as radar systems, supply their own source of energy to illuminate features of interest. These systems are termed "active" systems, in contrast to "passive" systems that sense naturally available energy. A very common example of an active system is a camera utilizing a flash. The same camera used in sunlight becomes a passive sensor.
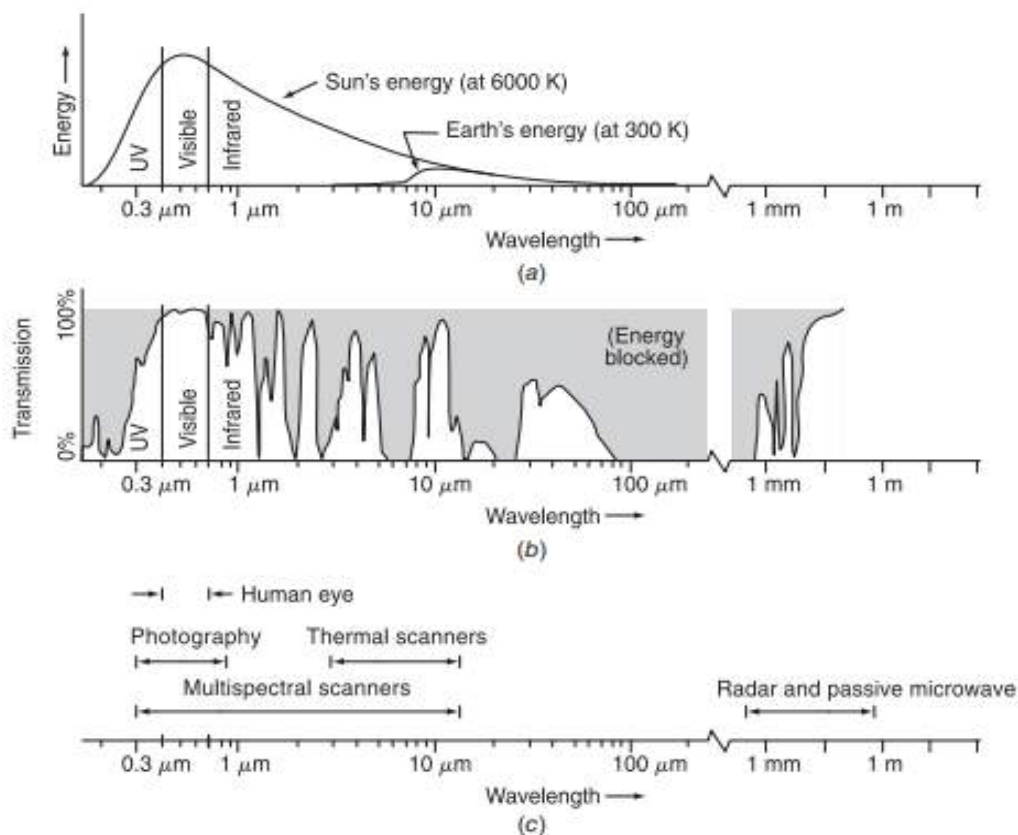
## 1.3 ENERGY INTERACTIONS IN THE ATMOSPHERE

Irrespective of its source, all radiation detected by remote sensors passes through some distance, or path length, of atmosphere. The path length involved can vary widely. For example, space photography results from sunlight that passes through the full thickness of the earth's atmosphere twice on its journey from source to sensor. On the other hand, an airborne thermal sensor detects energy emitted directly from objects on the earth, so a single, relatively short atmospheric path length is involved. The net effect of the atmosphere varies with these differences in path length and also varies with the magnitude of the energy signal being sensed, the atmospheric conditions present, and the wavelengths involved. Here, we merely wish to introduce the notion that the atmosphere can have a profound effect on, among other things, the intensity and spectral composition of radiation available to any sensing system. These effects are caused principally through the mechanisms of atmospheric scattering and absorption.

### *Absorption*

In contrast to scatter, atmospheric absorption results in the effective loss of energy to atmospheric constituents. This normally involves absorption of energy at a given wavelength. The most efficient absorbers of solar radiation in this regard are water vapor, carbon dioxide, and ozone. Because these gases tend to absorb electromagnetic energy in specific wavelength bands, they strongly influence the design of any remote sensing system. The wavelength ranges in which the atmosphere is particularly transmissive of energy are referred to as atmospheric windows. Figure 1.5 shows the interrelationship between energy sources and atmospheric absorption characteristics. Figure 2a shows the spectral distribution of the energy emitted by the sun and by earth features. These two curves represent the most common sources of energy used in remote sensing. In Figure 2b, spectral regions in which the atmosphere blocks energy are shaded. Remote sensing data acquisition is limited to the nonblocked spectral regions, the atmospheric windows. Note in Figure 1.5c that the spectral sensitivity range of the eye (the "visible" range) coincides with both an atmospheric window and the peak level of energy from the sun. Emitted "heat"

energy from the earth, shown by the small curve in (a), is sensed through the windows at 3 to 5 ᵐm and 8 to 14 ᵐm using such devices as thermal sensors. Multispectral sensors observe simultaneously through multiple, narrow wavelength ranges that can be located at various points in the visible through the thermal spectral region. Radar and passive microwave systems operate through a window in the region 1 mm to 1 m. The important point to note from Figure 2 is the interaction and the interdependence between the primary sources of electromagnetic energy, the atmospheric windows through which source energy may be transmitted to and from earth surface features, and the spectral sensitivity of the sensors available to detect and record the energy. One cannot select the sensor to be used in any given remote sensing task arbitrarily; one must instead consider (1) the spectral sensitivity of the sensors available, (2) the presence or absence of atmospheric windows in the spectral range(s) in which one wishes to sense, and (3) the source, magnitude, and spectral composition of the energy available in these ranges. Ultimately, however, the choice of spectral range of the sensor must be based on the manner in which the energy interacts with the features under investigation. It is to this last, very important, element that we now turn our attention.



**Figure 2:** Spectral characteristics of (*a*) energy sources, (*b*) atmospheric transmittance, and (*c*) common remote sensing systems. (Note that wavelength scale is logarithmic.)

## 1.4 Energy Interactions with Earth Surface Features

When electromagnetic energy is incident on any given earth surface feature, three fundamental energy interactions with the feature are possible. These are illustrated in Figure 1.6 for an element of the volume of a water body. Various fractions of the energy incident on the element are reflected, absorbed, and/or transmitted. Applying the principle of conservation of energy, we can state the interrelationship among these three energy interactions as
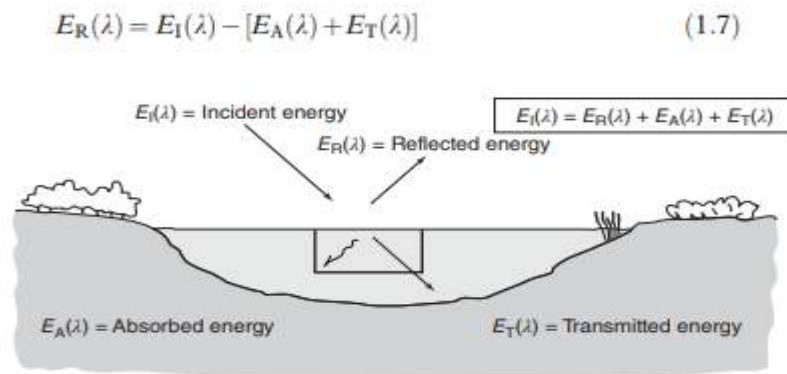
$$E_I(\lambda) = E_R(\lambda) + E_A(\lambda) + E_T(\lambda) \tag{1.6}$$

where

$E_I$ = incident energy
$E_R$ = reflected energy
$E_A$ = absorbed energy
$E_T$ = transmitted energy

with all energy components being a function of wavelength $\lambda$.

Equation 1.6 is an energy balance equation expressing the interrelationship among the mechanisms of reflection, absorption, and transmission. Two points concerning this relationship should be noted. First, the proportions of energy reflected, absorbed, and transmitted will vary for different earth features, depending on their material type and condition. These differences permit us to distinguish different features on an image. Second, the wavelength dependency means that, even within a given feature type, the proportion of reflected, absorbed, and transmitted energy will vary at different wavelengths. Thus, two features may be indistinguishable in one spectral range and be very different in another wavelength band. Within the visible portion of the spectrum, these spectral variations result in the visual effect called color. For example, we call objects "blue" when they reflect more highly in the blue portion of the spectrum, "green" when they reflect more highly in the green spectral region, and so on. Thus, the eye utilizes spectral variations in the magnitude of reflected energy to discriminate between various objects. Because many remote sensing systems operate in the wavelength regions in which reflected energy predominates, the reflectance properties of earth features are very important. Hence, it is often useful to think of the energy balance relationship expressed by Eq. 1.6 in the form

Anbar University – Engineering College          Subject: Remote Sensing
Dams and Water resources Eng. Dept.          Stage: Four
Dr. Ahmed Saud Mohammed , Dr. Khamis N. Syle

------------------------------------------------------------------------------------------------

$$E_R(\lambda) = E_I(\lambda) - [E_A(\lambda) + E_T(\lambda)] \tag{1.7}$$



Figure 3 Basic interactions between electromagnetic energy and an earth surface feature.

That is, the reflected energy is equal to the energy incident on a given feature reduced by the energy that is either absorbed or transmitted by that feature. The reflectance characteristics of earth surface features may be quantified by measuring the portion of incident energy that is reflected. This is measured as a function of wavelength and is called spectral reflectance, $\rho\lambda$. It is mathematically defined as

$$\rho_\lambda = \frac{E_R(\lambda)}{E_I(\lambda)}$$

$$= \frac{\text{energy of wavelength } \lambda \text{ reflected from the object}}{\text{energy of wavelength } \lambda \text{ incident upon the object}} \times 100 \tag{1.8}$$

where $\rho\lambda$ is expressed as a percentage.

A graph of the spectral reflectance of an object as a function of wavelength is termed a spectral reflectance curve. The configuration of spectral reflectance curves gives us insight into the spectral characteristics of an object and has a strong influence on the choice of wavelength region(s) in which remote sensing data are acquired for a particular application.

# The Third Lesson

## Spectral Reflectance of Earth Surface Feature Types.

Typical spectral reflectance curves for many different types of features as shown in Figure 1; healthy green grass, dry (non-photosynthetically active) grass, bare soil (brown to dark-brown sandy loam), pure gypsum dune sand, asphalt, construction concrete (Portland cement concrete), fine-grained snow, clouds, and clear lake water. The lines in this figure represent average reflectance curves compiled by measuring a large sample of features, or in some cases representative reflectance measurements from a single typical example of the feature class. Note how distinctive the curves are for each feature. In general, the configuration of these curves is an indicator of the type and condition of the features to which they apply. Although the reflectance of individual features can vary considerably above and below the lines shown here, these curves demonstrate some fundamental points concerning spectral reflectance. For example, spectral reflectance curves for healthy green vegetation almost always manifest the "peak-and-valley" configuration illustrated by green grass in Figure 1. The valleys in the visible portion of the spectrum are dictated by the pigments in plant leaves. Chlorophyll, for example, strongly absorbs energy in the wavelength bands centered at about 0.45 and 0:67 µm (often called the "chlorophyll absorption bands"). Hence, our eyes perceive healthy vegetation as green in color because of the very high absorption of blue and red energy by plant leaves and the relatively high reflection of green energy. If a plant is subject to some form of stress that interrupts its normal growth and productivity, it may decrease or cease chlorophyll production. The result is less chlorophyll absorption in the blue and red bands. Often, the red reflectance increases to the point that we see the plant turn yellow (combination of green and red). This can be seen in the spectral curve for dried grass in Figure 1.

 As we go from the visible to the near-IR portion of the spectrum, the reflectance of healthy vegetation increases dramatically. This spectral feature, known as the red edge, typically occurs between 0.68 and 0.75 µm, with the exact position depending on the species and condition. Beyond this edge, from about 0.75 to 1.3 µm (representing most of the near-IR range), a plant leaf typically reflects 40 to 50% of the energy incident upon it. Most of the remaining energy is transmitted, because absorption in this spectral region is minimal (less than 5%). Plant reflectance from 0.75 to 1.3 µm results primarily from the internal structure of plant leaves. Because the position of the red edge and the magnitude of the near-IR reflectance beyond the red edge are highly variable among plant species, reflectance measurements in these ranges often permit us to discriminate between species, even if they look the same in visible wavelengths. Likewise, many plant stresses alter the reflectance in the red edge and the near-IR region,

and sensors operating in these ranges are often used for vegetation stress detection. Also, multiple layers of leaves in a plant canopy provide the opportunity for multiple transmissions and reflections. Hence, the near-IR reflectance increases with the number of layers of leaves in a canopy, with the maximum reflectance achieved at about eight leaf layers (Bauer et al., 1986).
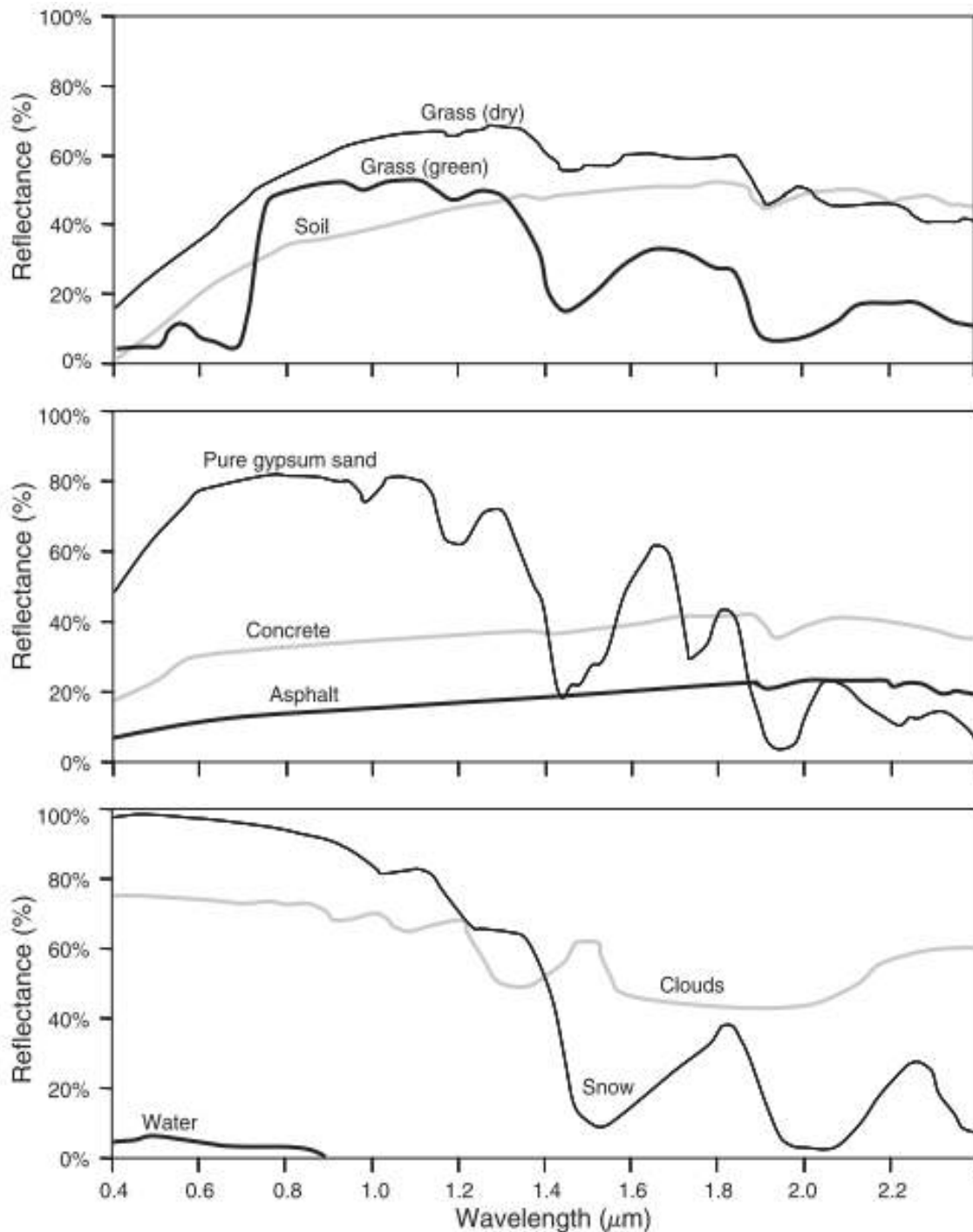


**Figure 1** Spectral reflectance curves for various features types. (Original data courtesy USGS Spectroscopy Lab, Johns Hopkins University Spectral Library, and Jet Propulsion Laboratory [JPL]; cloud spectrum from Bowker et al., after Avery and Berlin, 1992. JPL spectra © 1999, California Institute of Technology.)

Beyond 1.3 µm, energy incident upon vegetation is essentially absorbed or reflected, with little to no transmittance of energy. Dips in reflectance occur at 1.4, 1.9, and 2.7 µm because water in the leaf absorbs strongly at these wavelengths. Accordingly, wavelengths in these spectral regions are referred to as water absorption bands. Reflectance peaks occur at about 1.6 and 2.2 µm, between the absorption bands. Throughout the range beyond 1.3 µm, leaf reflectance is approximately inversely related to the total water present in a leaf. This total is a function of both the moisture content and the thickness of a leaf.

The soil curve in Figure 1.9 shows considerably less peak-and-valley variation in reflectance. That is, the factors that influence soil reflectance act over less specific spectral bands. Some of the factors affecting soil reflectance are moisture content, organic matter content, soil texture (proportion of sand, silt, and clay), surface roughness, and presence of iron oxide. These factors are complex, variable, and interrelated. For example, the presence of moisture in soil will decrease its reflectance. As with vegetation, this effect is greatest in the water absorption bands at about 1.4, 1.9, and 2.7 µm (clay soils also have hydroxyl absorption bands at about 1.4 and 2:2 µm). Soil moisture content is strongly related to the soil texture: Coarse, sandy soils are usually well drained, resulting in low moisture content and relatively high reflectance; poorly drained fine-textured soils will generally have lower reflectance. Thus, the reflectance properties of a soil are consistent only within particular ranges of conditions. Two other factors that reduce soil reflectance are surface roughness and content of organic matter. The presence of iron oxide in a soil will also significantly decrease reflectance, at least in the visible wavelengths. In any case, it is essential that the analyst be familiar with the conditions at hand. Finally, because soils are essentially opaque to visible and infrared radiation, it should be noted that soil reflectance comes from the uppermost layer of the soil and may not be indicative of the properties of the bulk of the soil.

 Sand can have wide variation in its spectral reflectance pattern. The curve shown in Figure 1.9 is from a dune in New Mexico and consists of roughly 99% gypsum with trace amounts of quartz (Jet Propulsion Laboratory, 1999). Its absorption and reflectance features are essentially identical to those of its parent material, gypsum. Sand derived from other sources, with differing mineral compositions, would have a spectral reflectance curve indicative of its parent material. Other factors affecting the spectral response from sand include the presence or absence of water and of organic matter. Sandy soil is subject to the same considerations listed in the discussion of soil reflectance.

As shown in Figure 1.9, the spectral reflectance curves for asphalt and Portland cement concrete are much flatter than those of the materials discussed thus far. Overall, Portland cement concrete tends to be relatively brighter than asphalt, both in the visible spectrum and at longer wavelengths. It is important to note that the reflectance of these materials may be modified by the presence of paint, soot, water, or other substances. Also, as materials age, their spectral reflectance patterns may change. For example, the reflectance of many types of asphaltic concrete may increase, particularly in the visible spectrum, as their surface ages.

In general, snow reflects strongly in the visible and near infrared, and absorbs more energy at mid-infrared wavelengths. However, the reflectance of snow is affected by its grain size, liquid water content, and presence or absence of other materials in or on the snow surface (Dozier and Painter, 2004). Larger grains of snow absorb more energy, particularly at wavelengths longer than 0.8 µm. At temperatures near 0°C, liquid water within the snowpack can cause grains to stick together in clusters, thus increasing the effective grain size and decreasing the reflectance at near-infrared and longer wavelengths. When particles of contaminants such as dust or soot are deposited on snow, they can significantly reduce the surface's reflectance in the visible spectrum.

The aforementioned absorption of mid-infrared wavelengths by snow can permit the differentiation between snow and clouds. While both feature types appear bright in the visible and near infrared, clouds have significantly higher reflectance than snow at wavelengths longer than 1.4 µm. Meteorologists can also use both spectral and bidirectional reflectance patterns (discussed later in this section) to identify a variety of cloud properties, including ice/water composition and particle size.

Considering the spectral reflectance of water, probably the most distinctive characteristic is the energy absorption at near-IR wavelengths and beyond. In short, water absorbs energy in these wavelengths whether we are talking about water features per se (such as lakes and streams) or water contained in vegetation or soil. Locating and delineating water bodies with remote sensing data are done most easily in near-IR wavelengths because of this absorption property. However, various conditions of water bodies manifest themselves primarily in visible wavelengths. The energy–matter interactions at these wavelengths are very complex and depend on a number of interrelated factors. For example, the reflectance from a water body can stem from an interaction with the water's surface (specular reflection), with material suspended in the water, or with the bottom of the depression containing the water body. Even with deep water where bottom effects are negligible, the reflectance properties of a water body are a function of not only the water per se but also the material in the water.

Clear water absorbs relatively little energy having wavelengths less than about 0.6 µm. High transmittance typifies these wavelengths with a maximum in the

blue-green portion of the spectrum. However, as the turbidity of water changes (because of the presence of organic or inorganic materials), transmittance— and therefore reflectanc—changes dramatically. For example, waters containing large quantities of suspended sediments resulting from soil erosion normally have much higher visible reflectance than other "clear" waters in the same geographic area. Likewise, the reflectance of water changes with the chlorophyll concentration involved. Increases in chlorophyll concentration tend to decrease water reflectance in blue wavelengths and increase it in green wavelengths. These changes have been used to monitor the presence and estimate the concentration of algae via remote sensing data. Reflectance data have also been used to determine the presence or absence of tannin dyes from bog vegetation in lowland areas and to detect a number of pollutants, such as oil and certain industrial wastes.

# The Forth Lesson

## Spectral Response for clear water

Many important water characteristics, such as dissolved oxygen concentration, pH, and salt concentration, cannot be observed directly through changes in water reflectance. However, such parameters sometimes correlate with observed reflectance. In short, there are many complex interrelationships between the spectral reflectance of water and particular characteristics. One must use appropriate reference data to correctly interpret reflectance measurements made over water.

Figure 1 illustrates some of these effects, using spectra from three lakes with different bio-optical properties. The first spectrum is from a clear, oligotrophic lake with a chlorophyll level of 1:2 ᵐ g/l and only 2.4 mg/l of dissolved organic carbon (DOC). Its spectral reflectance is relatively high in the blue-green portion of the spectrum and decreases in the red and near infrared. In contrast, the spectrum from a lake experiencing an algae bloom, with much higher chlorophyll concentration 12.3 ᵐ g/l, shows a reflectance peak in the green spectrum and absorption in the blue and red regions. These reflectance and absorption features are associated with several pigments present in algae. Finally, the third spectrum in Figure 1.10 was acquired on an ombrotrophic bog lake, with very high levels of DOC (20.7 mg/l). These naturally occurring tannins and other complex organic molecules give the lake a very dark appearance, with its reflectance curve nearly flat across the visible spectrum.
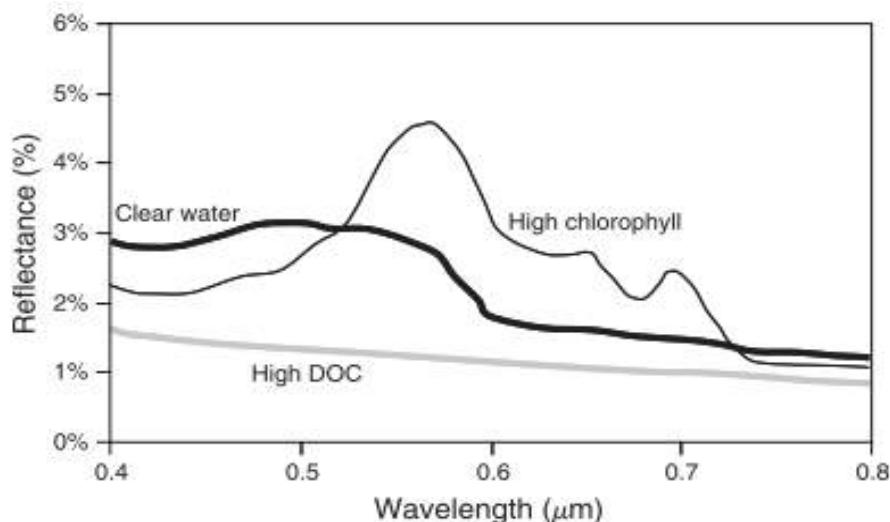


**Figure 1:** Spectral reflectance curves for lakes with clear water, high levels of chlorophyll, and high levels of dissolved organic carbon (DOC).

## Spectral Response Patterns

Having looked at the spectral reflectance characteristics of vegetation, soil, sand, concrete, asphalt, snow, clouds, and water, we should recognize that these broad feature types are often spectrally separable. However, the degree of separation between types varies among and within spectral regions. For example, water and vegetation might reflect nearly equally in visible wavelengths, yet these features are almost always separable in near-IR wavelengths.

Because spectral responses measured by remote sensors over various features often permit an assessment of the type and/or condition of the features, these responses have often been referred to as spectral signatures. Spectral reflectance and spectral emittance curves (for wavelengths greater than 3.0 $m$m) are often referred to in this manner. The physical radiation measurements acquired over specific terrain features at various wavelengths are also referred to as the spectral signatures for those features.

Although it is true that many earth surface features manifest very distinctive spectral reflectance and/or emittance characteristics, these characteristics result in spectral "response patterns" rather than in spectral "signatures." The reason for this is that the term signature tends to imply a pattern that is absolute and unique. This is not the case with the spectral patterns observed in the natural world. As we have seen, spectral response patterns measured by remote sensors may be quantitative, but they are not absolute. They may be distinctive, but they are not necessarily unique.

We have already looked at some characteristics of objects that influence their spectral response patterns. Temporal effects and spatial effects can also enter into any given analysis. Temporal effects are any factors that change the spectral characteristics of a feature over time. For example, the spectral characteristics of many species of vegetation are in a nearly continual state of change throughout a growing season. These changes often influence when we might collect sensor data for a particular application.

Spatial effects refer to factors that cause the same types of features (e.g., corn plants) at a given point in time to have different characteristics at different geographic locations. In small-area analysis the geographic locations may be meters apart and spatial effects may be negligible. When analyzing satellite data, the locations may be hundreds of kilometers apart where entirely different soils, climates, and cultivation practices might exist.

Temporal and spatial effects influence virtually all remote sensing operations. These effects normally complicate the issue of analyzing spectral reflectance properties of earth resources. Again, however, temporal and spatial effects might be the keys to gleaning the information sought in an analysis. For example, the process of change detection is premised on the ability to measure temporal effects. An example of this process is detecting the change in suburban development near a metropolitan area by using data obtained on two different dates.

**Atmospheric Influences on Spectral Response Patterns**

In addition to being influenced by temporal and spatial effects, spectral response patterns are influenced by the atmosphere. Regrettably, the energy recorded by a sensor is always modified to some extent by the atmosphere between the sensor and the ground. Figure 2 provides an initial frame of reference for understanding the nature of atmospheric effects. Shown in this figure is the typical situation encountered when a sensor records reflected solar energy. The atmosphere affects the "brightness," or radiance, recorded over any given point on the ground in two almost contradictory ways. First, it attenuates (reduces) the energy illuminating a ground object (and being reflected from the object). Second, the atmosphere acts as a reflector itself, adding a scattered, extraneous path radiance to the signal detected by the sensor. By expressing these two atmospheric effects mathematically, the total radiance recorded by the sensor may be related to the reflectance of the ground object and the incoming radiation or irradiance using the equation

$$L_{tot} = \frac{\rho E T}{\pi} + L_p \qquad (1.9)$$

*where*

$L_{tot}$ = total spectral radiance measured by sensor
$\rho$ = reflectance of object
$E$ = irradiance on object, incoming energy
$T$ = transmission of atmosphere
$L_p$ = path radiance, from the atmosphere and not from the object
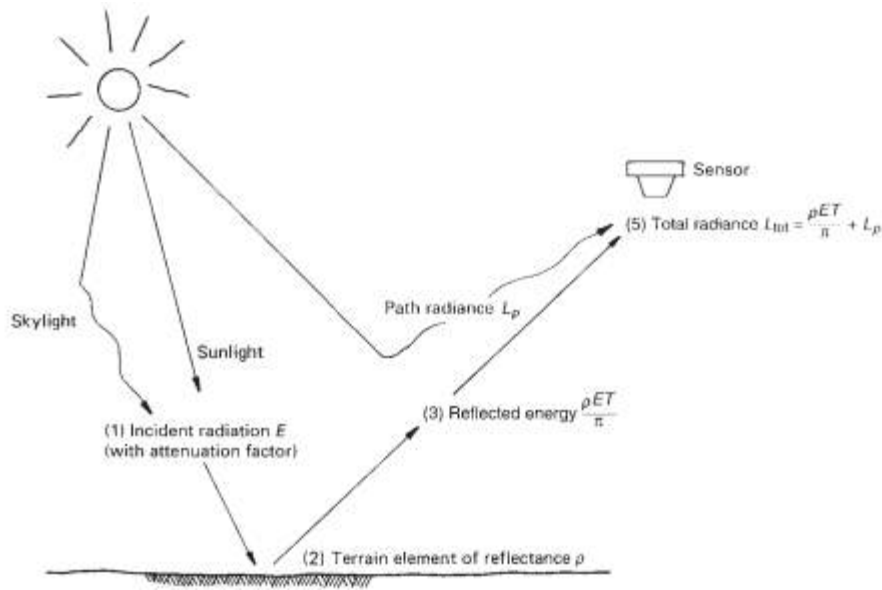
**Figure 2:** Atmospheric effects influencing the measurement of reflected solar energy.

It should be noted that all of the above factors depend on wavelength. Also, as shown in Figure 2 , the irradiance (E )stems from two sources: (1) directly reflected "sunlight" and (2) diffuse "skylight," which is sunlight that has been previously scattered by the atmosphere. The relative dominance of sunlight versus skylight in any given image is strongly dependent on weather conditions (e.g., sunny vs. hazy vs. cloudy). Likewise, irradiance varies with the seasonal changes in solar elevation angle (Figure 7.4) and the changing distance between the earth and sun.

For a sensor positioned close to the earth's surface, the path radiance $L_p$ will generally be small or negligible, because the atmospheric path length from the surface to the sensor is too short for much scattering to occur. In contrast, imagery from satellite systems will be more strongly affected by path radiance, due to the longer atmospheric path between the earth's surface and the spacecraft. This can be seen in Figure 3, which compares two spectral response patterns from the same area. One "signature" in this figure was collected using a handheld field spectroradiometer (see Section 1.6 for discussion), from a distance of only a few cm above the surface. The second curve shown in Figure 3 was collected by the Hyperion hyperspectral sensor on the EO-1 satellite (hyperspectral systems)
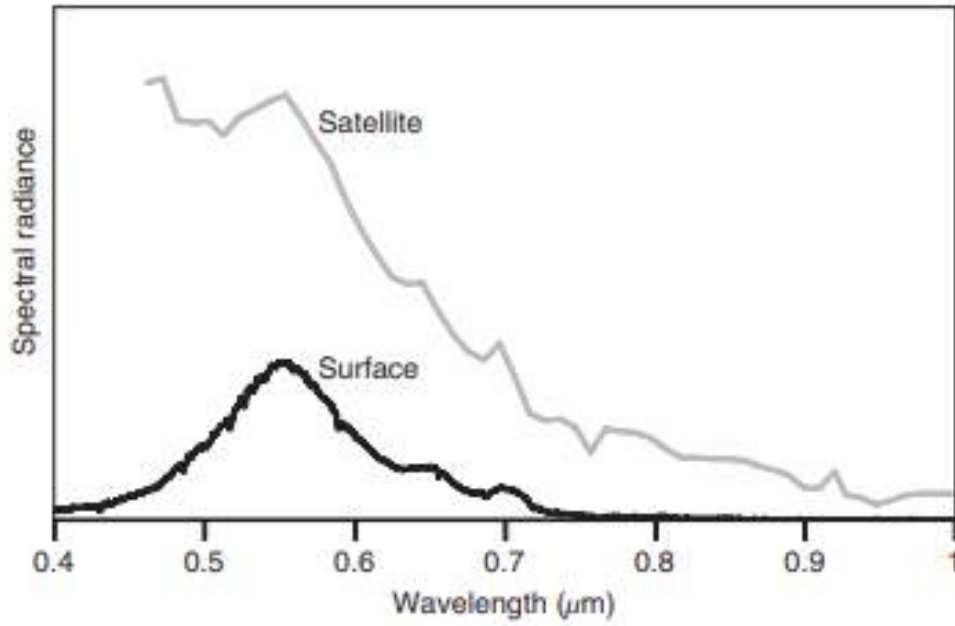
**Figure 3:** Spectral response patterns measured using a field spectroradiometer in close proximity to the earth's surface, and from above the top of the atmosphere (via the Hyperion instrument on EO-1). The difference between the two "signatures" is caused by atmospheric scattering and absorption in the Hyperion image.

# The Fifth Lesson

## Data Acquisition and Digital Image Concepts

To this point, we have discussed the principal sources of electromagnetic energy, the propagation of this energy through the atmosphere, and the interaction of this energy with earth surface features. These factors combine to produce energy "signals" from which we wish to extract information. We now consider the procedures by which these signals are detected, recorded, and interpreted.

The detection of electromagnetic energy can be performed in several ways. Before the development and adoption of electronic sensors, analog film-based cameras used chemical reactions on the surface of a light-sensitive film to detect energy variations within a scene. By developing a photographic film, we obtained a record of its detected signals. Thus, the film acted as both the detecting and the recording medium.

These pre-digital photographic systems offered many advantages:
- They were relatively simple and inexpensive
- provided a high degree of spatial detail and geometric integrity.

Electronic sensors generate an electrical signal that corresponds to the energy variations in the original scene. A familiar example of an electronic sensor is a handheld digital camera. Different types of electronic sensors have different designs of detectors, ranging from charge-coupled devices (CCDs) to the antennas used to detect microwave signals .

Regardless of the type of detector, the resulting data are generally recorded onto some magnetic or optical computer storage medium, such as a hard drive, memory card, solid-state storage unit or optical disk. Although sometimes more complex and expensive than film based systems, electronic sensors offer the advantages of a broader spectral range of sensitivity, improved calibration potential, and the ability to electronically store and transmit data.

In remote sensing, the term photograph historically was reserved exclusively for images that were detected as well as recorded on film. The more generic term image was adopted for any pictorial representation of image data. Thus, a pictorial record from a thermal scanner (an electronic sensor) would be called a "thermal image," not a "thermal photograph," because film would not be the original detection mechanism for the image.
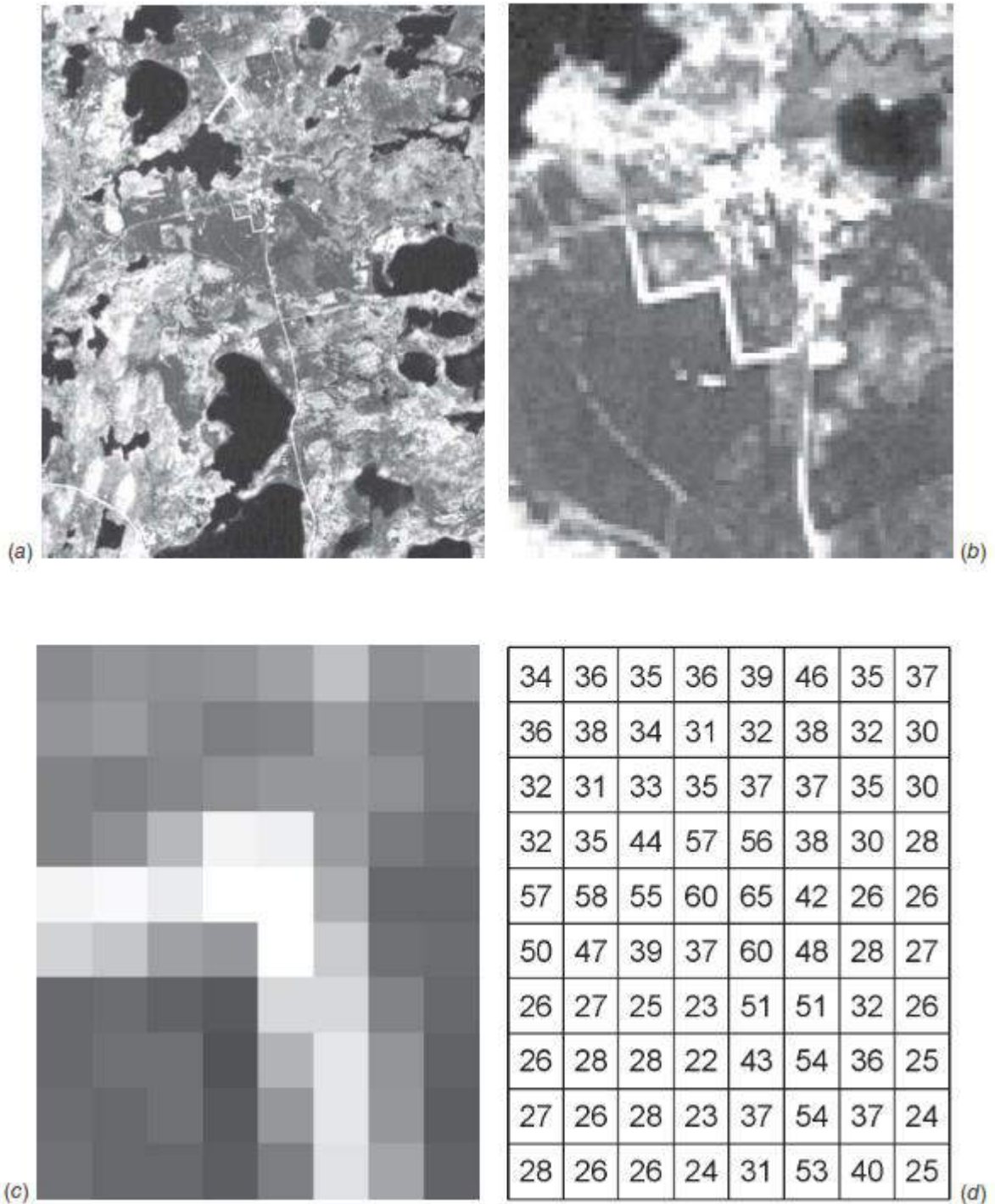
Because the term image relates to any pictorial product, all photographs are images. Not all images, however, are photographs. A common exception to the above terminology is use of the term digital pho-tography. As we describe in Section 2.5, digital cameras use electronic detectors rather than film for image detection. While this process is not "photography" in the traditional sense, "digital photography" is now the common way to refer to this technique of digital data collection.

We can see that the data interpretation aspects of remote sensing can involve analysis of pictorial (image) and/or digital data. Visual interpretation of pictorial image data has long been the most common form of remote sensing. Visual techniques make use of the excellent ability of the human mind to qualitatively evaluate spatial patterns in an image.

Visual interpretation techniques have certain disadvantages, however, in that they may require extensive training and are labor intensive. In addition, spectral characteristics are not always fully evaluated in visual interpretation efforts. This is partly because of the limited ability of the eye to discern tonal values on an image and the difficulty of simultaneously analyzing numerous spectral images. In applications where spectral patterns are highly informative, it is therefore preferable to analyze digital, rather than pictorial, image data.

The basic character of digital image data is illustrated in Figure 1. Although the image shown in (a) appears to be a continuous-tone photograph, it is actually composed of a two-dimensional array of discrete picture elements, or pixels. The intensity of each pixel corresponds to the average brightness, or radiance, measured electronically over the ground area corresponding to each pixel. A total of 500 rows and 400 columns of pixels are shown in Figure 1.a. Whereas the individual pixels are virtually impossible to discern in (a), they are readily observable in the enlargements shown in (b) and (c).

These enlargements correspond to sub-areas located near the center of (a). A 100 row 3 80 column enlargement is shown in (b) and a 10 row 3 8 column enlargement is included in (c). Part (d) shows the individual digital number (DN)—also referred to as the "brightness value" or "pixel value"—corresponding to the average radiance measured in each pixel shown in (c).

| 34 | 36 | 35 | 36 | 39 | 46 | 35 | 37 |
|----|----|----|----|----|----|----|----|
| 36 | 38 | 34 | 31 | 32 | 38 | 32 | 30 |
| 32 | 31 | 33 | 35 | 37 | 37 | 35 | 30 |
| 32 | 35 | 44 | 57 | 56 | 38 | 30 | 28 |
| 57 | 58 | 55 | 60 | 65 | 42 | 26 | 26 |
| 50 | 47 | 39 | 37 | 60 | 48 | 28 | 27 |
| 26 | 27 | 25 | 23 | 51 | 51 | 32 | 26 |
| 26 | 28 | 28 | 22 | 43 | 54 | 36 | 25 |
| 27 | 26 | 28 | 23 | 37 | 54 | 37 | 24 |
| 28 | 26 | 26 | 24 | 31 | 53 | 40 | 25 |

**Figure 1 :** Basic character of digital image data. (*a*) Original 500 row 3 400 column digital image. Scale 1:200,000. (*b*) Enlargement showing 100 row 3 80 column area of pixels near center of (*a*). Scale 1:40,000. (*c*) 10 row 3 8 column enlargement. Scale 1:4,000. (*d*) Digital numbers corresponding to the radiance of each pixel shown in (*c*). (Author-prepared figure.)

These values result from quantizing the original electrical signal from the sensor into positive integer values using a process called analog-to-digital (A-to-D) signal conversion.

Whether an image is acquired electronically or photographically, it may contain data from a single spectral band or from multiple spectral bands. The image shown in Figure 1 was acquired using a single broad spectral band, by integrating all energy measured across a range of wavelengths (a process analogous to photography using "black-and-white" film). Thus, in the digital image, there is a single DN for each pixel. It is also possible to collect "color" or multispectral imagery, whereby data are collected simultaneously in several spectral bands.

In the case of a color photograph, three separate sets of detectors (or, for analog cameras, three layers within the film) each record radiance in a different range of wavelengths.

In the case of a digital multispectral image, each pixel includes multiple DNs, one for each spectral band. For example, as shown in Figure 2, one pixel in a digital image might have values of 88 in the first spectral band, perhaps representing blue wavelengths, 54 in the second band (green), 27 in the third (red), and so on, all associated with a single ground area.

When viewing this multi-band image, it is possible to view a single band at a time, treating it as if it were a discrete image, with brightness values proportional to DN as in Figure 1.

Alternatively, and more commonly, three bands from the image can be selected and displayed simultaneously in shades of red, green, and blue, to create a color composite image, whether on a computer monitor or in a hard copy print. If the three bands being displayed were originally detected by the sensor in the red, green, and blue wavelength ranges of the visible spectrum, then this composite will be referred to as a true-color image, because it will approximate the natural combination of colors that would be seen by the human eye.

Any other combination of bands—perhaps involving bands acquired in wavelengths outside the visible spectrum—will be referred to as a false-color image. One common false-color combination of spectral bands involves displaying near-IR, red, and green bands (from the sensor) in red, green, and blue, respectively, on the display device.

Note that, in all cases, these three-band composite images involve displaying some combination of bands from the sensor in red, green, and blue on the display device because the human eye perceives color as a mixture of these three primary colors.

With multi-band digital data, the question arises of how to organize the data. In many cases, each band of data is stored as a separate file or as a separate block of data within a single file.
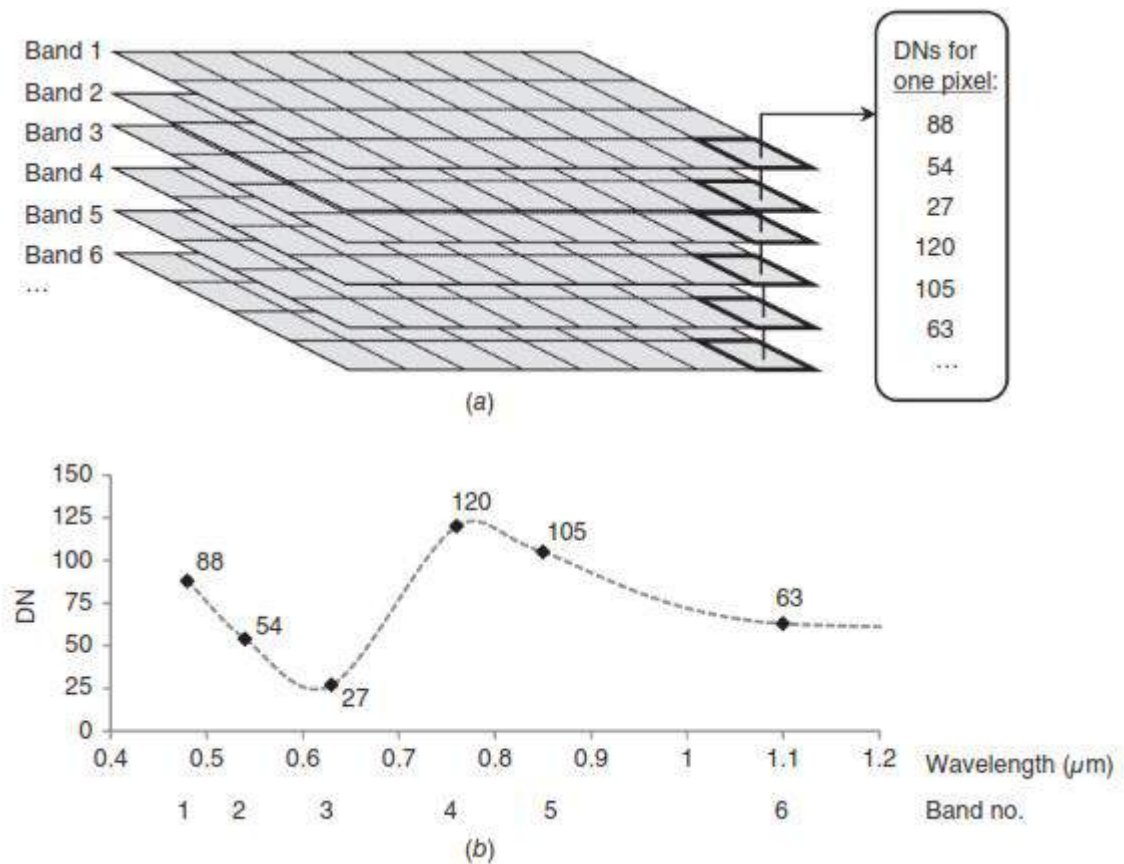


**Figure 2:** Basic character of multi-band digital image data. (*a*) Each band is represented by a grid of cells or pixels; any given pixel has a set of DNs representing its value in each band. (*b*) The spectral signature for the pixel highlighted in (*a*), showing band number and wavelength on the X axis and pixel DN on the Y axis. Values between the wavelengths of each spectral band, indicated by the dashed line in (*b*), are not measured by this sensor and would thus be unknown.

This format is referred to as band sequential (BSQ) format. It has the advantage of simplicity, but it is often not the optimal choice for efficient display and visualization of data, because viewing even a small portion of the image requires reading multiple blocks of data from different "places" on the computer disk. For example, to view a true-color digital image in BSQ for- mat, with separate files used to store the red, green, and blue spectral bands, it would be necessary for the computer to read blocks of data from three locations on the storage medium.

An alternate method for storing multi-band data utilizes the band interleaved by line (BIL) format. In this case, the image data file contains first a line of data from band 1, then the same line of data from band 2, and each subsequent band. This block of data consisting of the first line from each band is then followed by the second line of data from bands 1, 2, 3, and so forth.

The third common data storage format is band interleaved by pixel (BIP). This is perhaps the most widely used format for three-band images, such as those from most consumer-grade digital cameras. In this format, the file contains each band's measurement for the first pixel, then each band's measurement for the next pixel, and so on. The advantage of both BIL and BIP formats is that a computer can read and process the data for small portions of the image much more rapidly, because the data from all spectral bands are stored in closer proximity than in the BSQ format.

Typically, the DNs constituting a digital image are recorded over such numerical ranges as 0 to 255, 0 to 511, 0 to 1023, 0 to 2047, 0 to 4095 or higher. These ranges represent the set of integers that can be recorded using 8-, 9-, 10-, 11-, and 12-bit binary computer coding scales, respectively. (That is, $2^8 = 256$, $2^9 = 512$, $2^{10} = 1024$, $2^{11} = 2048$, $2^{12} = 4096$).

The technical term for the number of bits used to store digital image data is quantization level (or color depth, when used to describe the number of bits used to display a color image). As discussed in Chapter 7, with the appropriate calibration coefficients these integer DNs can be converted to more meaningful physical units such as spectral reflectance, radiance, or normalized radar cross section.

# The Sixth Lesson

**Elevation Data**

Increasingly, remote sensing instruments are used to collect three-dimensional spatial data, in which each observation has a Z coordinate representing elevation, along with the X and Y coordinates used to represent the horizontal position of the pixel's column and row. Particularly when collected over broad areas, these elevation data may represent the topography, the three-dimensional shape of the land surface. In other cases (usually, at finer spatial scales), these elevation data may represent the three-dimensional shapes of objects on or above the ground surface, such as tree crowns in a forest, or buildings in a city.

Elevation data may be derived from the analysis of raw measurements from many types of remote sensing instruments, including photographic systems, multispectral sensors, radar systems, and lidar systems.Elevation data may be represented in many different formats.

Figure 1.a shows a small portion of a traditional contour map, from the U.S. Geological Survey's 7.5-minute (1:24,000-scale) quadrangle map series. In this map, topographic elevations are indicated by contour lines. Closely spaced lines indicate steep terrain, while flat areas like river floodplains have more widely spaced contours.

Figure 1.b shows a digital elevation model (DEM). Note that the white rectangle in (b) represents the much smaller area shown in (a). The **DEM** is similar to a digital image, with the DN at each pixel representing a surface elevation rather than a radiance value. In (b), the brightness of each pixel is represented as being proportional to its elevation, so light-toned areas are topographically higher and dark-toned areas are lower. The region shown in this map consists of highly dissected terrain, with a complex network of river valleys; one major valley runs from the upper right portion of (b) to the lower center, with many tributary valleys branching off from each side. Figure 1.c shows another way of visualizing topographic data using shaded relief.
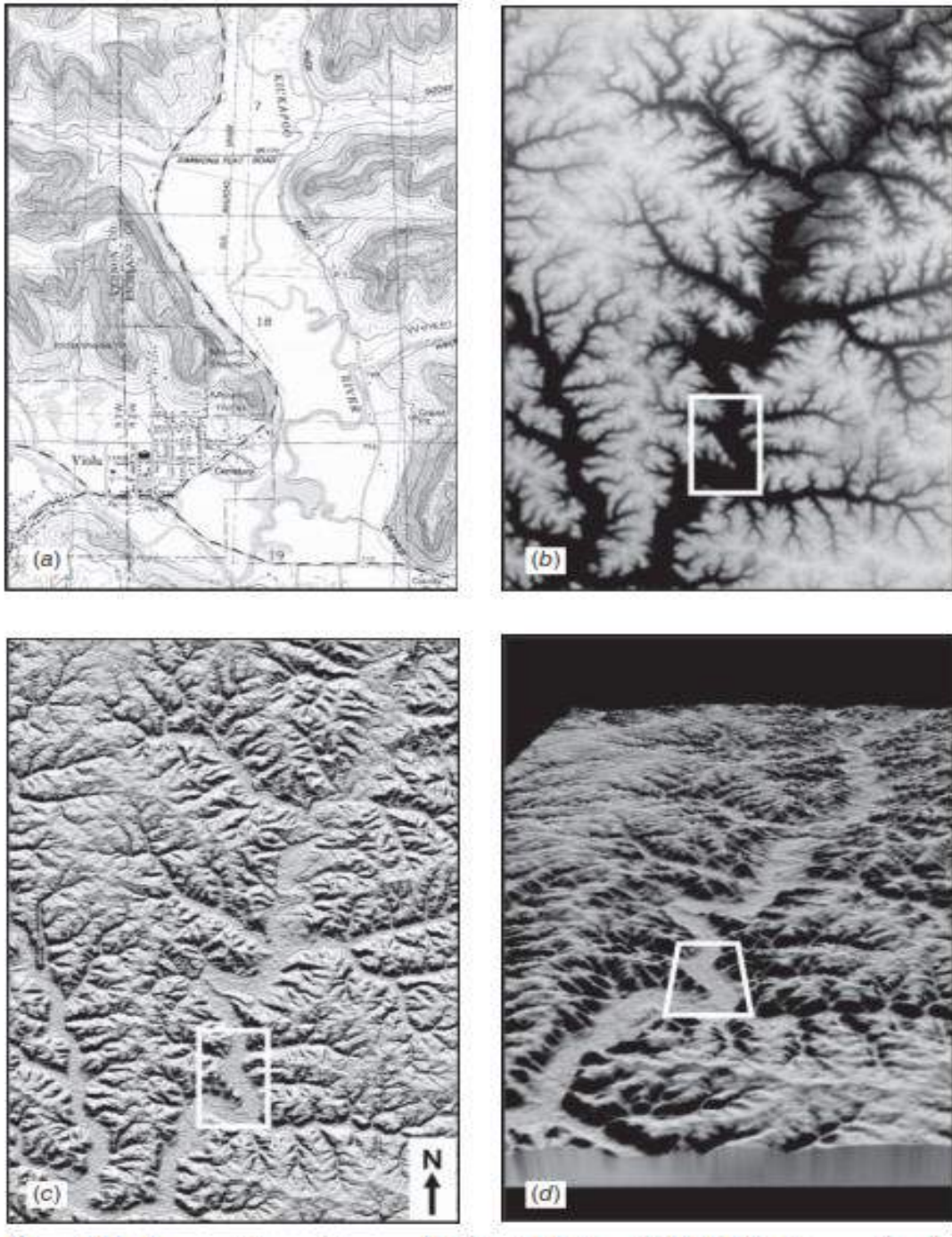
**Figure 1:** Representations of topographic data. (*a*) Portion of USGS 7.5-minute quadrangle map, showing elevation contours. Scale 1:45,000. (*b*) Digital elevation model, with brightness proportional to elevation. Scale 1:280,000. (*c*) Shaded-relief map derived from (*b*), with simulated illumination from the north. Scale 1:280,000. (*d*) Three-dimensional perspective view, with shading derived from (*c*). Scale varies in this projection. White rectangles in (*b*), (*c*), and (*d*) indicate area enlarged in (*a*). (Author-prepared figure.)

This is a simulation of the pattern of shading that would be expected from a three-dimensional surface under a given set of illumination conditions. In this case, the simulation includes a primary source of illumination located to the north, with a moderate degree of diffuse illumination from other directions to soften the intensity of the shadows. Flat areas will have uniform tone in a shaded relief map. Slopes facing toward the simulated light source will appear bright, while slopes facing away from the light will appear darker.

To aid in visual interpretation, it is often preferable to create shaded relief maps with illumination from the top of the image, regardless of whether that is a direction from which solar illumination could actually come in the real world. When the illumination is from other directions, particularly from the bottom of the image, an untrained analyst may have difficulty correctly perceiving the landscape; in fact, the topography may appear inverted.

Figure 1.d shows yet another method for visualizing elevation data, a three dimensional perspective view. In this example, the shaded relief map shown in (c) has been "draped" over the DEM, and a simulated view has been created based on a viewpoint located at a specified position in space (in this case, above and to the south of the area shown). This technique can be used to visualize the appearance of a landscape as seen from some point of interest. It is possible to "drape" other types of imagery over a DEM; perspective views created using an aerial photograph or high-resolution satellite image may appear quite realistic.

Animation of successive perspective views created along a user-defined flight line permits the development of simulated "fly-throughs" over an area. The term "digital elevation model" or DEM can be used to describe any image where the pixel values represent elevation $Z$ coordinates.

Two common subcategories of DEMs are a digital terrain model (DTM) and a digital surface model (DSM). A DTM (sometimes referred to as a "bald-earth DEM") records the elevation of the bare land surface, without any vegetation, buildings, or other features above the ground. In contrast, a DSM records the elevation of whatever the uppermost surface is at every location; this could be a tree crown, the roof of a building, or the ground surface (where no vegetation or structures are present).

Each of these models has its appropriate uses. For example, a DTM would be useful for predicting runoff in a watershed after a rainstorm, because

streams will flow over the ground surface rather than across the top of the forest canopy.

In contrast, a DSM could be used to measure the size and shape of objects on the terrain, and to calculate intervisibility (whether a given point B can be seen from a reference point A). Figure 2 compares a DSM and DTM for the same site, using airborne lidar data from the Capitol Forest area in Washington State (Andersen, McGaughey, and Reutebuch, 2005).

In Figure 2 a, the uppermost lidar points have been used to create a DSM showing the elevation of the upper surface of the forest canopy, the presence of canopy gaps, and, in many cases, the shape of individual tree crowns.



(a)

(b)
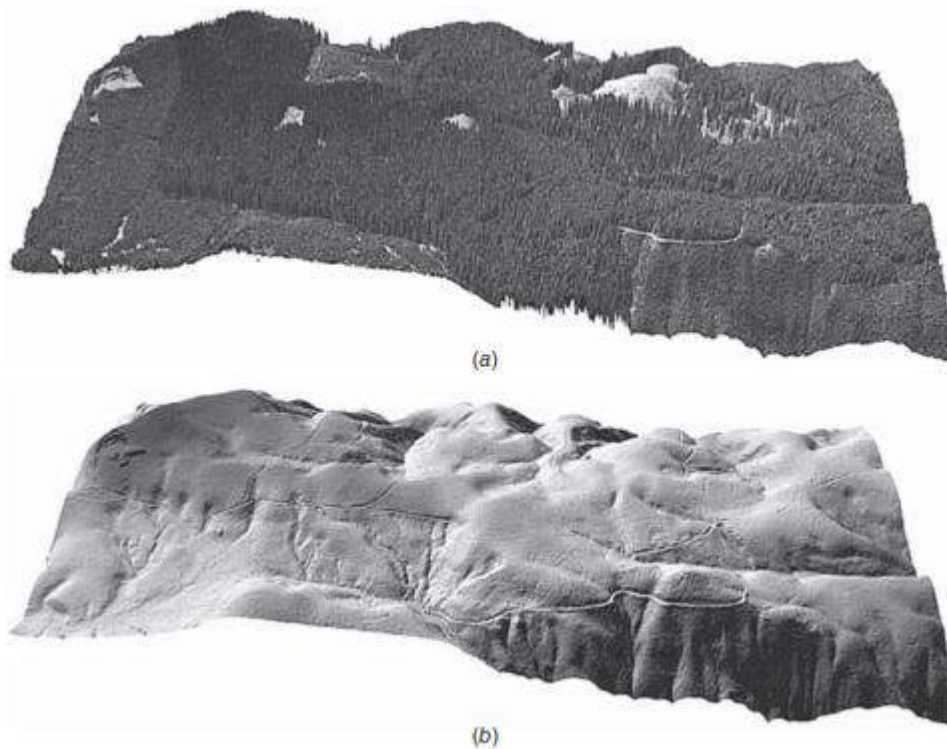
**Figure 2:** Airborne lidar data of the Capitol Forest site, Washington State. (*a*) Digital surface model (DSM) showing tops of tree crowns and canopy gaps. (*b*) Digital terrain model (DTM) showing hypothetical bare earth surface. (From Andersen et al., 2006; courtesy Ward Carlson, USDA Forest Service PNW Research Station.)

In Figure 2. b, the lowermost points have been used to create a DTM, showing the underlying ground surface if all vegetation and structures were

removed. Note the ability to detect fine-scale topographic features, such as small gullies and roadcuts, even underneath a dense forest canopy (Andersen et al., 2006).

Plate 1 shows a comparison of a DSM (a) and DTM (b) for a wooded area in New Hampshire. The models were derived from airborne lidar data acquired in early December. This site is dominated by a mix of evergreen and deciduous tree species, with the tallest (pines and hemlocks) exceeding 40 m in height. Scattered clearings in the center and right side are athletic fields, parkland, and former ski slopes now being taken over by shrubs and small trees. With obscuring vegetation removed, the DTM in (b) shows a variety of glacial and post-glacial landforms, as well as small roads, trails, and other constructed features.

Also, by subtracting the elevations in (b) from those in (a), it is possible to calculate the height of the forest canopy above ground level at each point. The result, shown in (c), is referred to as a canopy height model (CHM). In this model, the ground surface has been flattened, so that all remaining variation represents differences in height of the trees relative to the ground. Lidar and other high-resolution 3D data are widely used for this type of canopy height analysis (Clark et al., 2004).

Increasingly, elevation data are being used for analysis not just in the form of highly processed DEM, but in the more basic form of a point cloud. A point cloud is simply a data set containing many three-dimensional point locations, each representing a single measurement of the X, Y, Z coordinates of an object or surface. The positions, spacing, intensity, and other characteristics of the points in this cloud can be analyzed using sophisticated 3D processing algorithms to extract information about features (Rutzinger et al., 2008).

## Reference Data

As we have indicated in the previous discussion, rarely, if ever, is remote sensing employed without the use of some form of reference data. The acquisition of reference data involves collecting measurements or observations about the objects, areas, or phenomena that are being sensed remotely. These data can take on any of a number of different forms and may be derived from a number of sources. For example, the data needed for a particular analysis might be derived from a soil survey map, a water quality laboratory report, or an aerial photograph. They may also stem from

a "field check" on the identity, extent, and condition of agricultural crops, land uses, tree species, or water pollution problems.

Reference data may also involve field measurements of temperature and other physical and/or chemical properties of various features. The geographic positions at which such field measurements are made are often noted on a map base to facilitate their location in a corresponding remote sensing image. Usually, GPS receivers are used to determine the precise geographic position of field observations and measurements .

Reference data are often referred to by the term ground truth. This term is not meant literally, because many forms of reference data are not collected on the ground and can only approximate the truth of actual ground conditions. For example, "ground" truth may be collected in the air, in the form of detailed aerial photographs used as reference data when analyzing less detailed high altitude or satellite imagery. Similarly, the "ground" truth will actually be "water" truth if we are studying water features. In spite of these inaccuracies, ground truth is a widely used term for reference data.

Reference data might be used to serve any or all of the following purposes:
1. To aid in the analysis and interpretation of remotely sensed data.
2. To calibrate a sensor.
3. To verify information extracted from remote sensing data.

Hence, reference data must be collected in accordance with the principles of statistical sampling design appropriate to the particular application. Reference data can be very expensive and time consuming to collect properly. They can consist of either time-critical and/or time-stable measurements. Time- critical measurements are those made in cases where ground conditions change rapidly with time, such as in the analysis of vegetation condition or water pollution events.

Time-stable measurements are involved when the materials under observation do not change appreciably with time. For example, geologic applications often entail field observations that can be conducted at any time and that would not change appreciably from mission to mission.

One form of reference data collection is the ground-based measurement of the reflectance and/or emittance of surface materials to determine their spectral response patterns. This might be done in the laboratory or in the field using the principles of spectroscopy.

Spectroscopic measurement procedures can involve the use of a variety of instruments. Often, a spectroradiometer is used in such measurement procedures. This device measures, as a function of wavelength, the energy coming from an object within its view. It is used primarily to prepare spectral reflectance curves for various objects.

In laboratory spectroscopy, artificial sources of energy might be used to illuminate objects under study. In the laboratory, other field parameters such as viewing geometry between object and sensor are also simulated. More often, therefore, in situ field measurements are preferred because of the many variables of the natural environment that influence remote sensor data that are difficult, if not impossible, to duplicate in the laboratory.

In the acquisition of field measurements, spectroradiometers may be operated in a number of modes, ranging from handheld to helicopter or aircraft mounted . Figure 3 illustrates a highly portable instrument that is well suited for handheld operation. Through a fiber-optic input, this particular system acquires a continuous spectrum by recording data in over 1000 narrow bands simultaneously (over the range 0.35 to 2:5 mm). The unit is typically transported in a backpack carrier with provision for integrating the spectrometer with a notebook computer. The computer provides for flexibility in data acquisition, display, and storage. For example, reflectance spectra can be displayed in real time, as can computed reflectance values within the wavelength bands of various satellite systems.
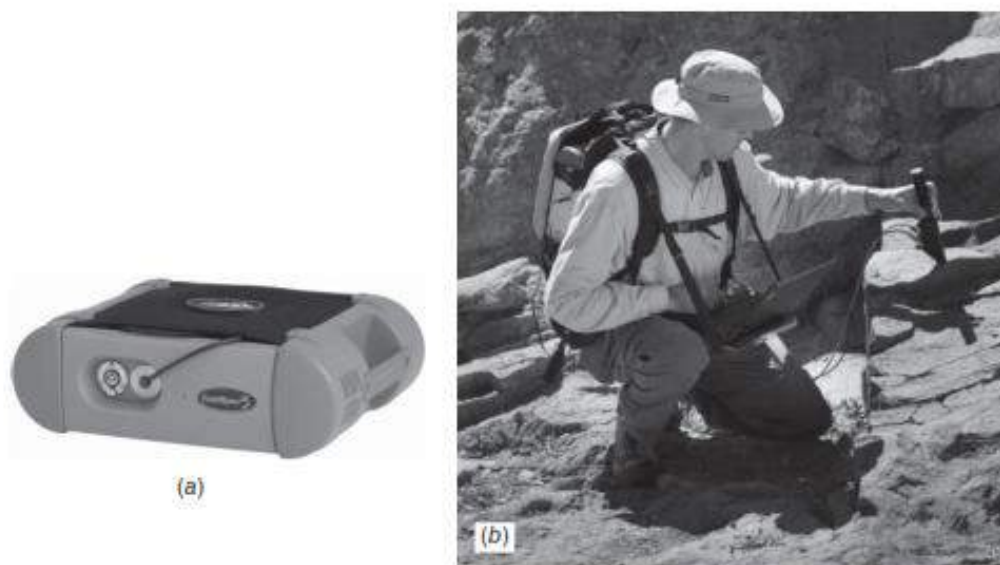


**Figure 3:** ASD, Inc. FieldSpec Spectroradiometer: (*a*) the instrument; (*b*) instrument shown in field operation. (Courtesy ASD, Inc.)

In-field calculation of band ratios and other computed values is also possible. One such calculation might be the normalized difference vegetation index (NDVI), which relates the near-IR and visible reflectance of earth surface features . Another option is matching measured spectra to a library of previously measured samples. The overall system is compatible with a number of post-processing software packages and also affords Ethernet, wireless, and GPS compatibility as well. Figure 4 shows a versatile all-terrain instrument platform designed primarily for collecting spectral measurements in agricultural cropland environments.

The system provides the high clearance necessary for making measurements over mature row crops, and the tracked wheels allow access to difficult landscape positions. Several measurement instruments can be suspended from the system's telescopic boom. Typically, these include a spectroradiometer, a remotely operated digital camera system, and a GPS receiver . While designed primarily for data collection in agricultural fields, the long reach of the boom makes this device a useful tool for collecting spectral data over such targets as emergent vegetation found in wetlands as well as small trees and shrubs. Using a spectroradiometer to obtain spectral reflectance measurements is normally a three-step process. First, the instrument is aimed at a calibration panel of known, stable reflectance. The purpose of this step is to quantify the incoming radiation, or irradiance, incident upon the measurement site. Next, the instrument is suspended over the target of interest and the radiation reflected by the object is measured.



**Figure 4:** All-terrain instrument platform designed for collecting spectral measurements in agricultural cropland environments. (Courtesy of the University of Nebraska-Lincoln Center for Advanced Land Management Information Technologies.)

Finally, the spectral reflectance of the object is computed by ratioing the reflected energy measurement in each band of observation to the incoming radiation measured in each band. Normally, the term reflectance factor is used to refer to the result of such computations.

A reflectance factor is defined formally as the ratio of the radiant flux actually reflected by a sample surface to that which would be reflected into the same sensor geometry by an ideal, perfectly diffuse (Lambertian) surface irradiated in exactly the same way as the sample.

Another term frequently used to describe the above type of measurement is bidirectional reflectance factor: one direction being associated with the sample viewing angle (usually 0° from normal) and the other direction being that of the sun's illumination (defined by the solar zenith and azimuth angles. In the bidirectional reflectance measurement procedure described above, the sample and the reflectance standard are measured sequentially. Other approaches exist in which the incident spectral irradiance and reflected spectral radiance are measured simultaneously.

# The Seventh Lesson

## Image Parallax

### Characteristics of Image Parallax

Thus far we have limited our discussion to photogrammetric operations involving only single vertical photographs. Numerous applications of photogrammetry incorporate the analysis of stereo pairs and use of the principle of parallax. The term parallax refers to the apparent change in relative positions of stationary objects caused by a change in viewing position. This phenomenon is observable when one looks at objects through a side window of a moving vehicle. With the moving window as a frame of reference, objects such as mountains at a relatively great distance from the window appear to move very little within the frame of reference. In contrast, objects close to the window, such as roadside trees, appear to move through a much greater distance.

In the same way that the close trees move relative to the distant mountains, terrain features close to an aircraft (i.e., at higher elevation) will appear to move relative to the lower elevation features when the point of view changes between successive exposures. These relative displacements form the basis for three dimensional viewing of overlapping photographs. In addition, they can be measured and used to compute the elevations of terrain points.

Figure 1 illustrates the nature of parallax on overlapping vertical photographs taken over varied terrain. Note that the relative positions of points A and B change with the change in viewing position (in this case, the exposure station). Note also that the parallax displacements occur only parallel to the line of flight.
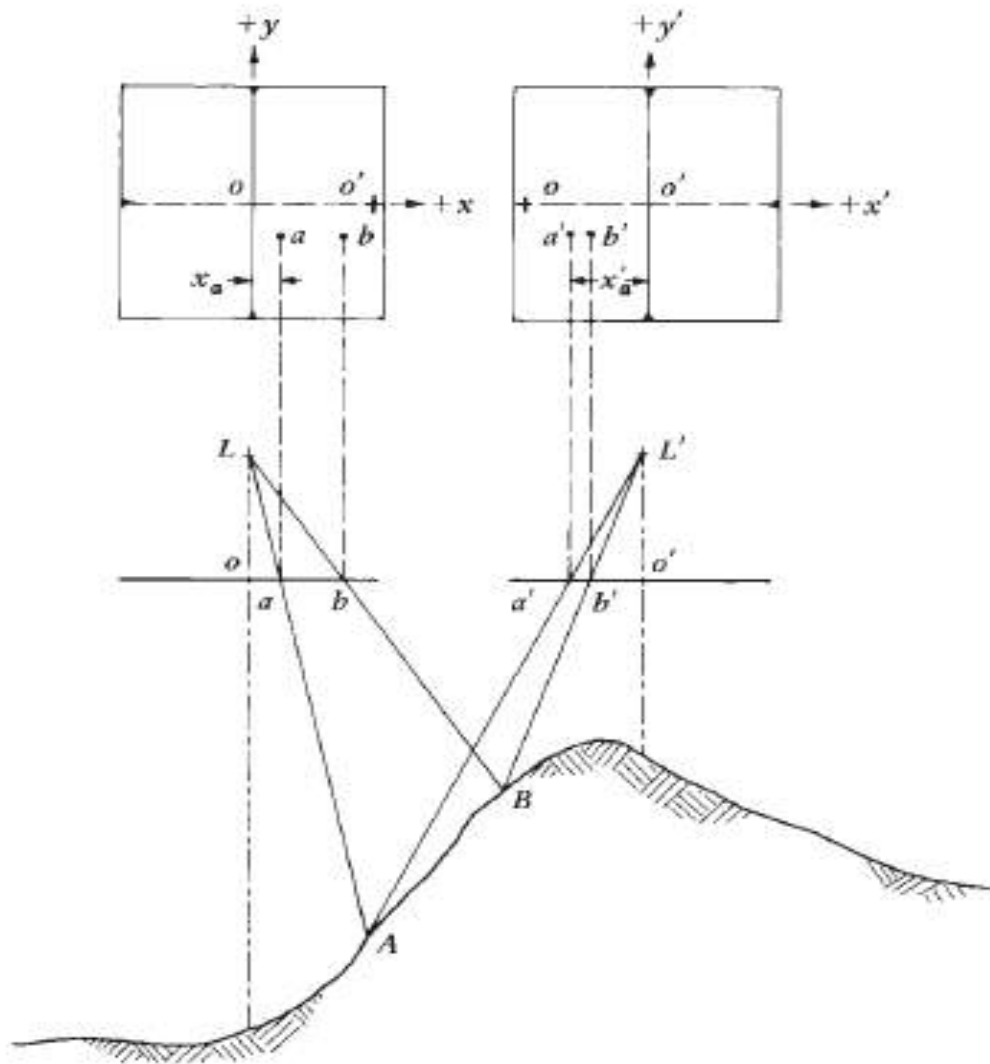
Figure 1  Parallax displacements on overlapping vertical photographs.

In theory, the direction of flight should correspond precisely to the fiducial x axis. In reality,however, unavoidable changes in the aircraft orientation will usually slightly offset the fiducial axis from the flight axis. The true flight line axis may be found by first locating on a photograph the points that correspond to the image centers of the preceding and succeeding photographs. These points are called the conjugate principal points. A line drawn through the principal points and the conjugate principal points defines the flight axis. As shown in Figure 2, all photographs except those on the ends of a flight strip normally have two sets of flight axes.

This happens because the aircraft's path between exposures is usually slightly curved. In Figure 3.15, the flight axis for the stereopair formed by

2

photos 1 and 2 is flight axis 12. The flight axis for the stereopair formed by photos 2 and 3 is flight axis 23.

The line of flight for any given stereopair defines a photocoordinate x axis for use in parallax measurement. Lines drawn perpendicular to the flight line and passing through the principal point of each photo form the photographic y axes for parallax measurement. The parallax of any point, such as A in Figure 2 , is expressed
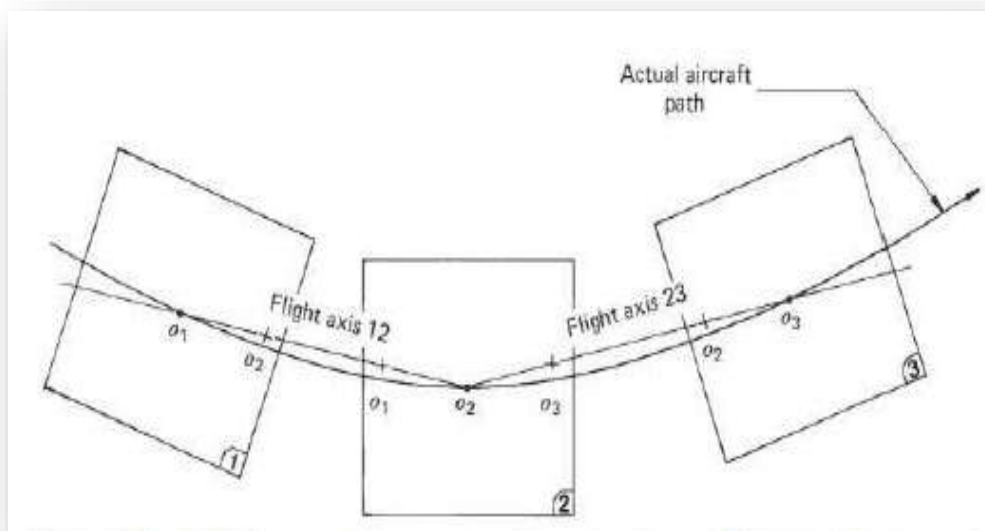


**Figure 2** Flight line axes for successive stereopairs along a flight strip. (Curvature of aircraft path is exaggerated.)

in terms of the flight line coordinate system as

$$p_a = x_a - x'_a \tag{3.8}$$

*where*

$p_a$ = parallax of point $A$
$x_a$ = measured $x$ coordinate of image $a$ on the left photograph of the stereopair
$x'_a$ = $x$ coordinate of image $a'$ on the right photograph

The $x$ axis for each photo is considered positive to the right of each photo principal point. This makes $x'_a$ a negative quantity in Figure 3.14.

Anbar University – Engineering College          Subject: Remote Sensing
Dams and Water resources Eng. Dept.          Stage: Four
          Dr. Ahmed Saud Mohammed , Dr. Khamis N. Syle
-----------------------------------------------------------------------------------------------------------

# The Eighth Lesson

### Object Height and Ground Coordinate Location from Parallax Measurement

Figure 1 shows overlapping vertical photographs of a terrain point, A. Using parallax measurements, we may determine the elevation at A and its ground coordinate location. Referring to Figure 1-a, the horizontal distance between exposure stations L and L0 is called B, the air base. The triangle in Figure 1b results from superimposition of the triangles at L and L0 in order to graphically depict the nature of parallax pa as computed from Eq. 3.8 algebraically. From similar triangles La0
xax (Figure 1 b) and LAxL0 (Figure a)

$$\frac{p_a}{f} = \frac{B}{H - h_A}$$

from which

$$H - h_A = \frac{Bf}{p_a} \tag{3.9}$$
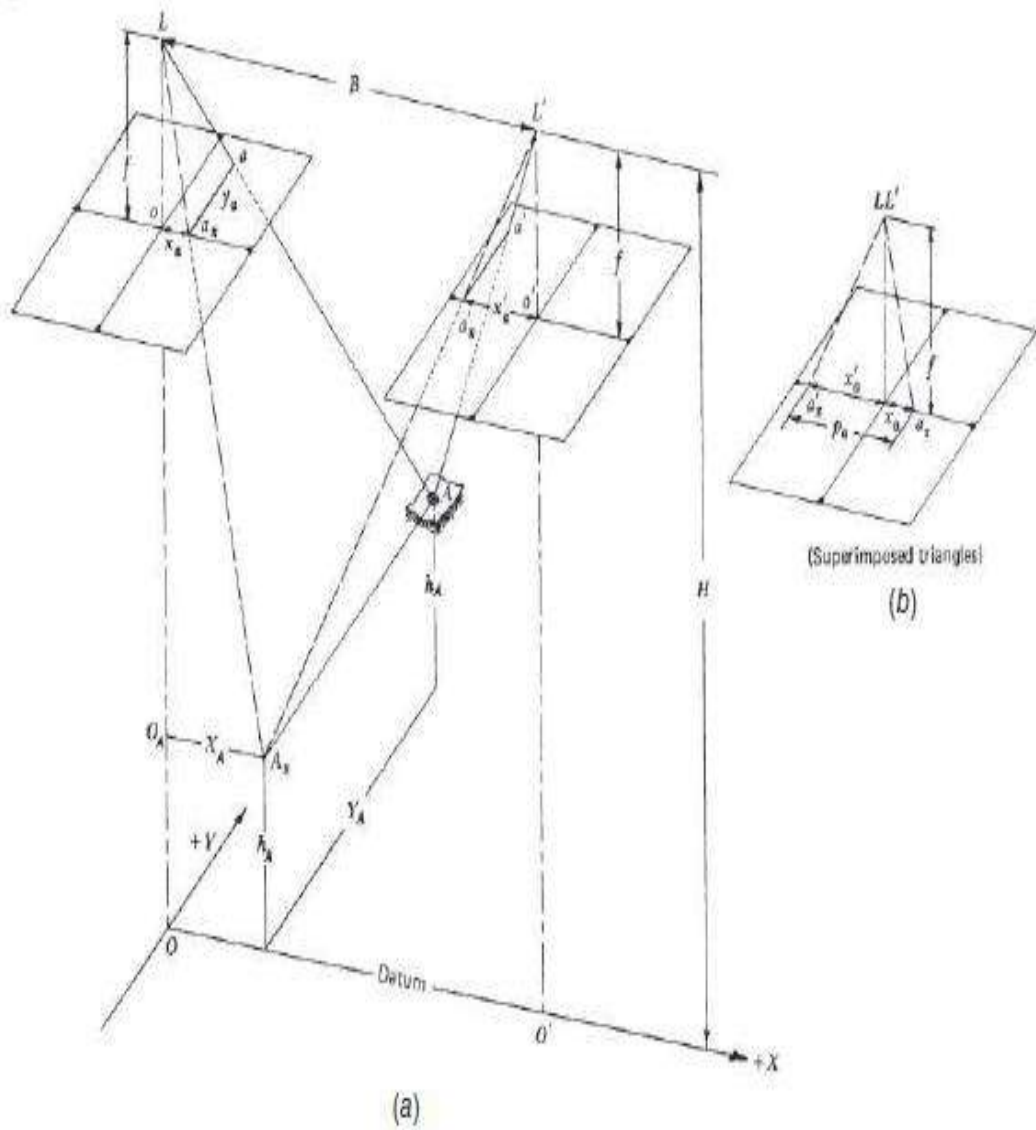
**Figure 1 :** Parallax relationships on overlapping vertical photographs: (*a*) adjacent photographs forming a stereopair; (*b*) superimposition of right photograph onto left.

Anbar University – Engineering College          Subject: Remote Sensing
Dams and Water resources Eng. Dept.          Stage: Four
        Dr. Ahmed Saud Mohammed , Dr. Khamis N. Syle
-----------------------------------------------------------------------------------------------------------

Rearranging yields

$$h_A = H - \frac{Bf}{p_a} \tag{3.10}$$

Also, from similar triangles $LO_A A_x$ and $Loa_x$,

$$\frac{X_A}{H - h_A} = \frac{x_a}{f}$$

from which

$$X_A = \frac{x_a(H - h_A)}{f}$$

and substituting Eq. 3.9 into the above equation yields

$$X_A = B\frac{x_a}{p_a} \tag{3.11}$$

A similar derivation using y coordinates yields

$$Y_A = B\frac{y_a}{p_a} \tag{3.12}$$

Equations 3.10 to 3.12 are commonly known as the parallax equations. In these equations, X and Y are ground coordinates of a point with respect to an arbitrary coordinate system whose origin is vertically below the left exposure station and with positive X in the direction of flight; p is the parallax of the point in question; and x and y are the photo coordinates of the point on the left-hand photo. The major assumptions made in the derivation of these equations are that the photos are truly vertical and that they are taken from the same flying height. If these assumptions are sufficiently met, a complete survey of the ground region contained in the photo overlap area of a stereo pair can be made.

Anbar University – Engineering College           Subject: Remote Sensing
Dams and Water resources Eng. Dept.            Stage: Four
Dr. Ahmed Saud Mohammed , Dr. Khamis N. Syle
-------------------------------------------------------------------------------------------------------------

**Flight Planning**

Frequently, the objectives of a photographic remote sensing project can only be met through procurement of new photography of a study area. These occasions can arise for many reasons. For example, photography available for a particular area could be outdated for applications such as land use mapping. In addition, available photography may have been taken in the wrong season. For example, photography acquired for topographic mapping is usually flown in the fall or spring to minimize vegetative cover. This photography will likely be inappropriate for applications involving vegetation analysis.

In planning the acquisition of new photography, there is always a trade-off between cost and accuracy. At the same time, the availability, accuracy, and cost of alternative data sources are continually changing as remote sensing technology advances. This leads to such decisions as whether analog or digital photography is appropriate. For many applications, high resolution satellite data may be an acceptable and cost-effective alternative to aerial photography. Similarly, lidar data might be used in lieu of, or in addition to, aerial photography. Key to making such decisions is specifying the nature and accuracy of the end product(s) required for the application at hand. For example, the required end products might range from hardcopy prints to DEMs, planimetric and topographic maps, thematic digital GIS datasets, and orthophotos, among many others.

The remainder of this discussion assumes that aerial photography has been judged to best serve the needs of a given project, and the task at hand is to develop a flight plan for acquiring the photography over the project＇s study area.

As previously mentioned, flight planning software is generally used for this purpose. Here we illustrate the basic computational considerations and procedures embedded in such software by presenting two "manual" example solutions to the flight planning process. We highlight the geometric aspects of preparing a flight plan for both a film-based camera mission and a digital camera mission of the same study area. Although we present two solutions using the same study area, we do not mean to imply that the two mission designs yield photography of identical quality and

utility. They are simply presented as two representative examples of the flight planning process.

Before we address the geometric aspects of photographic mission planning, we stress that one of the most important parameters in an aerial mission is beyond the control of even the best planner—the weather.

In most areas, only a few days of the year are ideal for aerial photography. In order to take advantage of clear weather, commercial aerial photography firms will fly many jobs in a single day, often at widely separated locations. Flights are usually scheduled between 10 a.m. and 2 p.m. for maximum illumination and minimum shadow, although digital cameras that provide high sensitivity under low light conditions can be used for missions conducted as late as sunset, or shortly thereafter, and under heavily overcast conditions. However, as previously mentioned, mission timing is often optimized to ensure strong GPS signals from a number of satellites, which may narrow the acquisition time window. In addition, the mission planner may need to accommodate such mission-specific constraints as maximum allowable building lean in orthophotos produced from the photography, occlusions in urban areas, specular reflections over areas covered by water, vehicular traffic volumes at the time of imaging, and civil and military air traffic control restrictions. Overall, a great deal of time, effort, and expense go into the planning and execution of a photographic mission.

In many respects, it is an art as well as a science. The parameters needed for the geometric design of a film-based photographic mission are (1) the focal length of the camera to be used, (2) the film format size,

(3) the photo scale desired, (4) the size of the area to be photographed, (5) the average elevation of the area to be photographed, (6) the overlap desired, (7) the sidelap desired, and (8) the ground speed of the aircraft to be used. When designing a digital camera photographic mission, the required parameters are the same, except the number and physical dimension of the pixels in the sensor array are needed in lieu of the film format size, and the GSD for the mission is required instead of a mission scale.

Based on the above parameters, the mission planner prepares computations and a flight map that indicate to the flight crew (1) the flying height above datum from which the photos are to be taken; (2) the location, direction, and number of flight lines to be made over the area to be photographed; (3) the time interval

between exposures; (4) the number of exposures on each flight line; and (5) the total number of exposures necessary for the mission.


When flight plans are computed manually, they are normally portrayed on a map for the flight crew. However, old photography or even a satellite image may be used for this purpose. The computations prerequisite to preparing flight plans for a film-based and a digital camera mission are given in the following two examples, respectively.

-----------------------------------------------------------------------------------------------------------------

# The Ninth Lesson

## Multispectral Scanners Systems

Multispectral imagery consists of image data selectively acquired in multiple spectral bands. The film-based, digital, and video camera systems might be considered as simple multispectral sensors, because they can be used to acquire imagery in three or four wavelength bands ranging from 0.3 to 0.9 µm. These instruments can be designed to collect data in many more spectral bands and over a wider range of the electromagnetic spectrum. Utilizing different types of electronic detectors, multispectral scanners can extend the range of sensing from 0.3 µm to approximately 14 µm. (This includes the UV, visible, near-IR, mid-IR, and thermal-IR spectral regions ).  Furthermore, multispectral scanner systems can sense in very narrow bands.

Many electronic (as opposed to photographic) remote sensors acquire data using scanning systems, which employ a sensor with a narrow field of view (i.e. IFOV) that sweeps over the terrain to build up and produce a two-dimensional image of the surface. Scanning systems can be used on both aircraft and satellite platforms and have essentially the same operating principles. A scanning system used to collect data over a variety of different wavelength ranges is called a multispectral scanner (MSS), and is the most commonly used scanning system. There are two main modes or methods of scanning employed to acquire multispectral image data - across-track scanning, and along-track scanning.
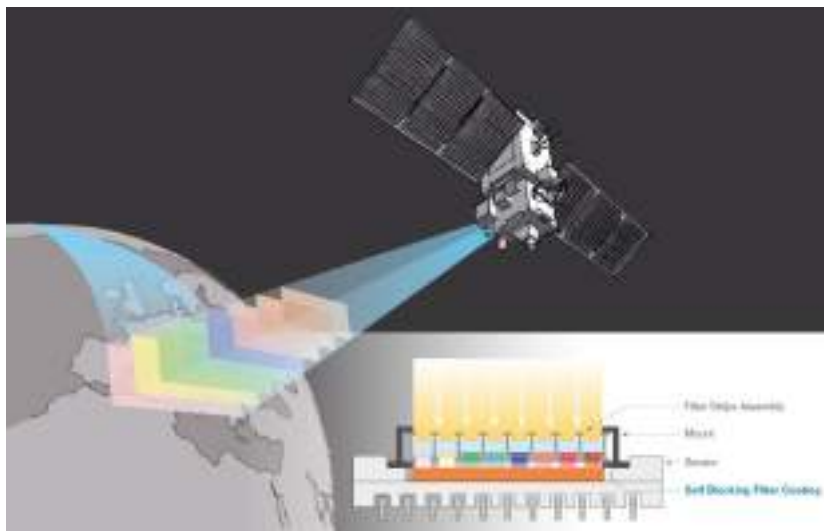


Figure 1: represent Remote Multi-Spectral Imaging

**Multispectral Remote Sensing**

In the visual interpretation of remotely sensed images, a variety of image characteristics are brought into consideration: color (or tone in the case of panchromatic images), texture, size, shape, pattern, context, and the like. However, with computer-assisted interpretation, it is most often simply color (i.e., the spectral response pattern) that is used. It is for this reason that a strong emphasis is placed on the use of multispectral sensors (sensors that, like the eye, look at more than one place in the spectrum and thus are able to gauge spectral response patterns), and the number and specific placement of these spectral *bands*.

Figure 2 illustrates the spectral bands of the LANDSAT Thematic Mapper (TM) system. The LANDSAT satellite is a commercial system providing multi-spectral imagery in seven spectral bands at a 30 meter resolution.



Band 1, visible blue 0.45-0.52 mm   Band 2, visible green 0.52-0.60 mm   Band 3, visible red 0.63-0.69 mm   Band 4, near-infrared 0.76-0.90 mm

Band 5, middle-infrared 1.55-1.75 mm   Band 6, thermal infrared 10.4-12.5 mm   Band 7, middle-infrared 2.08-2.35 mm
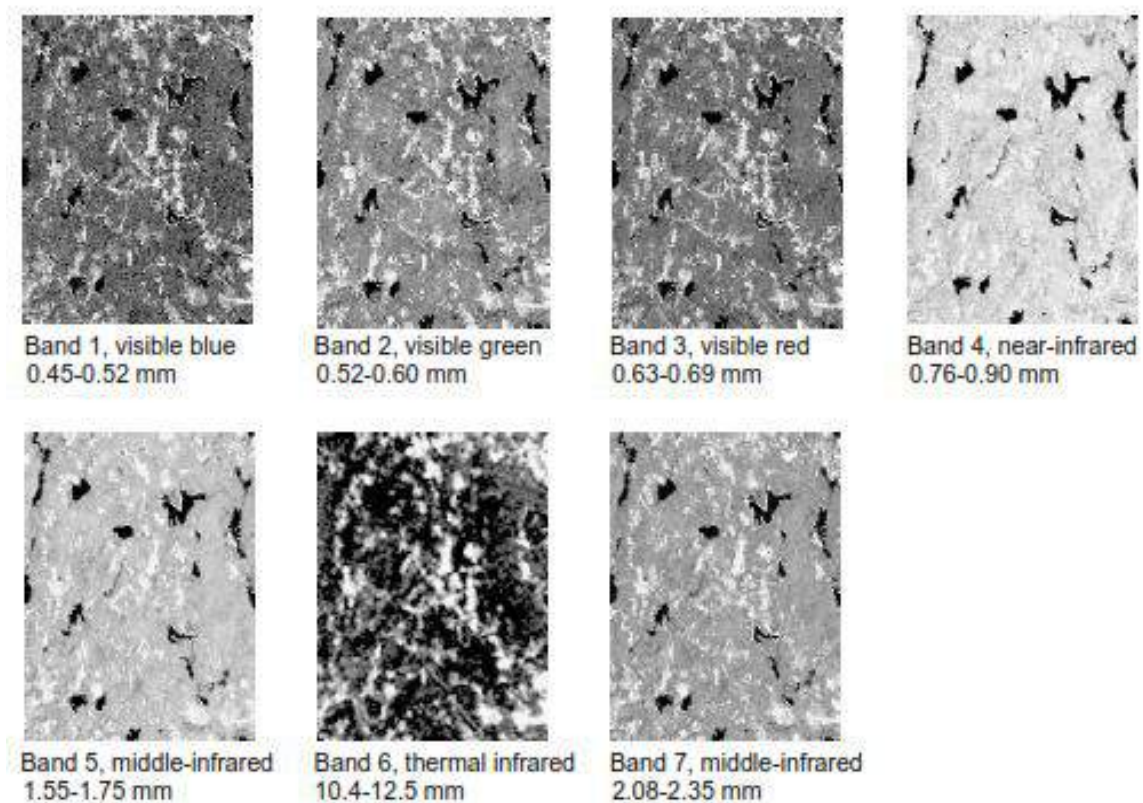
Figure 2: Represent multispectral images for same area

It can be shown through analytical techniques such as Principal Components Analysis, that in many environments, the bands that carry the

greatest amount of information about the natural environment are the near-infrared and red wavelength bands.

Water is strongly absorbed by infrared wavelengths and is thus highly distinctive  in that region. In addition, plant species typically show their greatest differentiation here. The red band is also very important because it is the primary region in which chlorophyll absorbs energy for photosynthesis. Thus it is this band which can most readily distinguish between vegetated and non-vegetated surfaces. Given this importance of the red and near-infrared bands, it is not surprising that sensor systems designed for earth resource monitoring will invariably include these in any particular multispectral system. Other bands will depend upon the range of applications envisioned.

Many include the green visible band since it can be used, along with the other two, to produce a traditional false color composite - a full color image derived from the green, red, and infrared bands (as opposed to the blue, green, and red bands of natural color images). This format became common with the advent of color infrared photography, and is familiar to many specialists in the remote sensing field. In addition, the combination of these three bands works well in the interpretation of the cultural landscape as well as natural and vegetated surfaces.

However, it is increasingly common to include other bands that are more specifically targeted to the differentiation of surface materials. For example, LANDSAT TM Band 5 is placed between two water absorption Bands and has thus proven very useful in determining soil and leaf moisture differences. Similarly, LANDSAT TM Band 7 targets the detection of hydrothermal alteration zones in bare rock surfaces. By contrast, the AVHRR  system on the NOAA series satellites includes several Thermal channels for the sensing of cloud temperature characteristics.
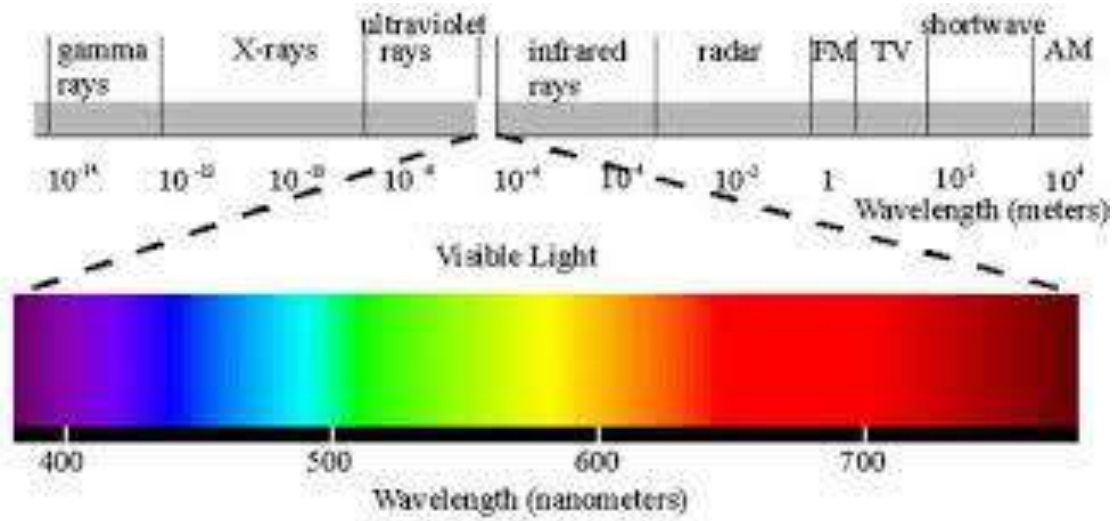
----------------------------------------------------------------------------------------------------



Figure 3: Represent Division of Visible band



Figure 4: Represent band combination of Images

# Hyperspectral Remote Sensing

In addition to traditional multispectral imagery, some new and experimental systems such as AVIRIS and MODIS are capable of capturing *hyperspectral* data. These systems cover a similar wavelength range to multispectral systems, but in much narrower bands. This dramatically increases the number of bands (and thus precision) available for image classification (typically tens and even Hundreds of very narrow bands). Moreover, hyperspectral signature libraries have been created in lab conditions and contain hundreds of signatures for different types of land covers, including many minerals and other earth materials.
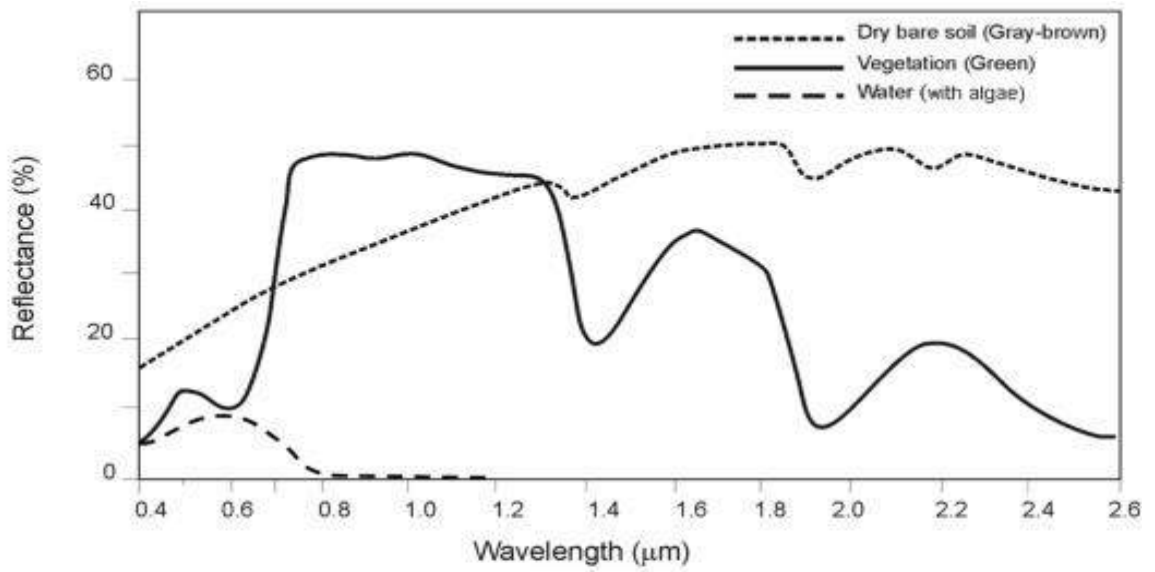
Thus, it should be possible to match signatures to surface materials with great precision. However, environmental conditions and natural variations in materials (which make them different from standard library materials) make this difficult. In addition, classification procedures have not been developed for hyperspectral data to the degree they have been for multispectral imagery. As a consequence, multispectral imagery still represents the major tool of remote sensing today.

# Landsat Series

The US space agency launched the first satellite of Landsat series (1-7)  in 1972 and was used in monitoring the Earth and environmental changes and then the rest of the satellites of the series were launched. These sensors were of three types:

- Return beam vidicon
- MultiSpectral Scanner
- Thematic mapper

Optical remote sensing makes use of visible, near infrared and short-waveinfrared sensors to form images of the earth's surface by detecting the solar radiation reflected from targets on the ground. Thus, the targets can be differentiated by their spectral reflectance signatures in the remotely sensed images as shown in Figure 5.

Figure 5: Represent Spectral Reflectance of Water , Soil and Vegetation

Anbar University – Engineering College                     Subject: Remote Sensing

Dams and Water resources Eng. Dept.                     Stage: Four

Dr. Ahmed Saud Mohammed , Dr. Khamis N. Syle

---------------------------------------------------------------------------------------------------------------

# The Tenth Lesson

## Characteristics of Landsat satellites 1-3

The Landsat series passes in oribits  9 degrees away from the poles , they orbit the Earth every 103 minutes, about 14 cycles a day. The satellites intersect the equator   at an angle of 9 degrees. To provide nearly complete coverage of the Earth's surface, these satellites take images at length equal 185-km

The first generation of Landsat satellites (1-3) contains two types of sensors:

1.  RBV (3-bands)
2.  Multi - Spectral Scanner (MSS) with four spectral bands

The following table shows the general specifications of the Landsat satellite series

Table 1 :  Landsat Series information

| Satellite | Launch | Decommissioned | Sensors |
|---|---|---|---|
| Landsat 1 | July 23, 1972 | January 6, 1978 | MSS/RBV |
| Landsat 2 | January 22, 1975 | July 27, 1983 | MSS/RBV |
| Landsat 3 | March 5, 1978 | September 7, 1983 | MSS/RBV |
| Landsat 4 | July 16, 1982 | June 15, 2001 | MSS/TM |
| Landsat 5 | March 1, 1984 | 2013 | MSS/TM |
| Landsat 6 | October 5, 1993 | Did not achieve orbit | ETM |
| Landsat 7 | April 15, 1999 | Operational | ETM+ |
| Landsat 8 | February 11, 2013 | Operational | OLI/TIRS |

Table 2:  MSS band designation

| Landsat 1,2,3 Spectral bands | Landsat 4,5 Spectral bands | Band range (µm) | Resolution m | Use |
|---|---|---|---|---|
| Band 4 (Green) | Band 1 (Green) | 0.5 - 0.6 | 80 | Sediment – laden water – delineates areas of shallow water |
| Band 5 (Red) | Band 2 (Red) | 0.6 – 0.7 | 80 | Cultural features |
| Band 6 (Near IR) | Band 3 (Near IR) | 0.7 – 0.8 | 80 | Vegetation boundary between land and water - landforms |
| Band 7 (Near IR) | Band 4 (Near IR) | 0.8 – 1.1 | 80 | Penetrates atmospheric haze best – emphasizes vegetation – Boundary between land and water - landforms |

## Landsat Characteristics (4, 5)

Landsat (4, 5) was launched in orbits near the pole in conjunction with the sun and was lowered to improve the spatial resolution of the sensors  , each satellite crossing the equator at 9:45 am and taking 99 minutes ( 14.5)  cycles per day, as shown in Table (1).

There are two types of Landsat sensors (4 and 5),

-   Multi-Spectral Scanner (MSS), and
-    Thematic Mapper  (TM).
-

    The Landsat (MSS, TM) sensor system (4, 5) captures the reflected and emitted radiation  from the Earth's surface in Visible and Near Infrared (NIR) .

Anbar University – Engineering College         Subject: Remote Sensing

Dams and Water resources Eng. Dept.         Stage: Four

Dr. Ahmed Saud Mohammed , Dr. Khamis N. Syle

-------------------------------------------------------------------------------------------------------------------

## Landsat satellites (6 and 7)

The space shuttle, which carried Landsat 6 was fail , was unable to reach orbit. After the successful launch of the Landsat 7 satellite, the improvements that added to Landsat 6 were transferred to Landsat 7. The Landsat 7 has an enhanced Enhanced Thematic Mapper (ETM +), which is similar to the TM sensor, but is more sophisticated, adding a new bancrometric band with a spatial accuracy of 15 and an infrared thermal band. It also has a higher radiometric accuracy and resolution Accuracy than the sensor (MSS). The following table shows the spectral domains of TM in Landsat (4, 5) and ETM +  In Landsat 7 which operates in seven waves, with the characteristics of each field.

Table 3 TM and ETM+ Band desingation

| Landsat 7 Spectral bands | Wavelength Micrometer | Resolution m | Use |
|---|---|---|---|
| Band 1 Blue -  Green | 0.45 – 0.52 | 30 | Bathymetric mapping; distinguishes soil from vegetation; deciduous from coniferous vegetation. |
| Band 2 - Green | 0.52 -0.61 | 30 | Emphasizes peak vegetation, which is useful for assessing plant vigor. |
| Band 3 – Red | 0.63 -0.69 | 30 | Emphasizes vegetation slopes. |
| Band 4 – Reflected IR | 0.76 – 0.90 | 30 | Emphasizes biomass content and shorelines. |
| Band 5 – Reflected IR | 1.55 1.75 | 30 | Discriminates moisture content of soil and vegetation; penetrates thin clouds. |
| Band 6 – Thermal | 10.4 – 12.5 | 120 | Useful for thermal mapping and estimated soil moisture. |
| Band 7 – Reflected IR | 2.08 – 2.35 | 30 | Useful for mapping hydrothermally altered rocks associated with mineral deposits. |
| Band 8 – Panchromatic | 0.52 - 0.90 | 15 | Useful in 'sharpening' multispectral images. |

# Landsat 8 –  LC08

Landsat 8 is an American Earth observation satellite launched on February 11, 2013  was launch  from Vandenberg Air Force Base, California on an Atlas-V rocket. The satellite carries the Operational Land Imager (OLI) and the Thermal Infrared Sensor (TIRS). It is the eighth satellite in the Landsat program; the seventh to reach orbit successfully. Originally called the Landsat Data Continuity Mission, it is a collaboration between NASA and the United States Geological Survey.

The Landsat 8 satellite orbits the  Earth in a sun-synchronous, near-polar orbit, at an altitude of 705 km (438 mi), inclined at 98.2 degrees, and circles the Earth every 99 minutes.  The satellite has a 16-day repeat cycle . Landsat 8 aquires about 740 scenes a day on the Worldwide Reference System-2 (WRS-2) path/row system, with a swath overlap (or sidelap) varying from 7 percent at the Equator to a maximum of approximately 85 percent at extreme latitudes. The scene size is 185 km x 180 km (114 mi x 112 mi).



Figure 6:  Landsat 8

Table 4:  Landsat 8 bands designation

| No of Band | Wavelength μm | Resolution m | Use |
|---|---|---|---|
| Band 1 (coastal/ Aerosol) | 0.435-0.451 | 30 | Increased coastal zone observations. |
| Band 2 - Blue | 0.452-0.512 | 30 | Bathymetric mapping; distinguishes soil from vegetation; deciduous from coniferous vegetation. |
| Band 3 - Green | 0.533-0.590 | 30 | Emphasizes peak vegetation, which is useful for assessing plant vigor. |
| Band 4 - Red | 0.636-0.673 | 30 | Emphasizes vegetation slopes. |
| Band 5 Near IR | 0.851-0.879 | 30 | Emphasizes vegetation boundary between land and water, and landforms. |
| Band 6 Short Wavelength Infrared | 1.566-1.651 | 30 | Used in detecting plant drought stress and delineating burnt areas and fire-affected vegetation, and is also sensitive to the thermal radiation emitted by intense fires; can be used to detect active fires, especially during nighttime when the background interference from SWIR in reflected sunlight is absent |
| Band 7 Short Wavelength Infrared | 2.107-2.294 | 30 | Used in detecting drought stress, burnt and fire-affected areas, and can be used to detect active fires, especially at nighttime. |

| | | | |
|---|---|---|---|
| Band 8<br><br>Panchrom-atic | 0.5 – 0.68 | 15 | Useful in 'sharpening' multispectral images. |
| Band 9<br>Cirrus =<br>Cloud | | 30 | Useful in detecting cirrus clouds. |
| Band 10<br><br>Thermal<br>Infrared  1 | 10.60-11.19 | 100 | Useful for mapping thermal differences in water currents, monitoring fires and other night<br>studies, and estimating soil moisture. |
| Band 11<br><br>Thermal<br>Infrared  2 | 11.50-12.51 | 100 | Useful for mapping thermal differences in water currents, monitoring fires and other night<br>studies, and estimating soil moisture. |

## SPOT Satellites Series

The first satellite of the Spot series was launched from the Court launch range in French Guiana in 1986, carrying the first Ground survey sensor, containing a linear matrix sensor . Spot features other programs with a light-emitting device, a linear array sensor and a holographic capability. After the launch of the first satellite of the Spot series in 1986, Spot (2) was launched in 1990, followed by Spot 3 in 1993, which stop in 1996, while Spot (1 and 2 still working in their orbits.

### Sensors on board SPOT 1 – 3

Spot has two high resolution visual (HRV)  and magnetic tape recorders. The camera employs two types of sensor systems:

# 1. Pancromatic mode (P)

 A wide spectral band, with the exception of blue, is sensed with a spatial resolution of up to 10 m. It is mainly intended for studies that require geometrical detail،

# 2. Mutiltispectral mode (XS)

 Three spectral bands are sensed:

- XS1 (0.50 – 0.59) μm (Green band)
- XS2(0.61-0.68) μm (Red Band)
- XS3(0.79 – 0.89) μm (NIR band)
  By gaining the  data recorded in this set of spectral beams, composite color images can be produced with a precision resolution of 20 m. The figure below shows the HRV sensor in Spot Satellite
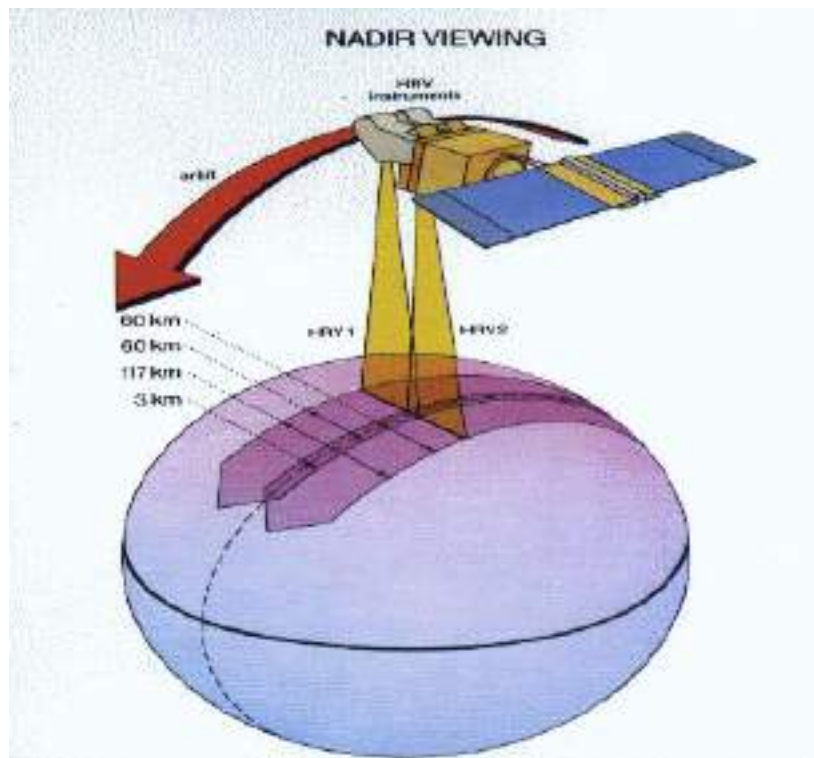


Figure 7: represent Landsat SPOT